



## Mitochondrial remodeling underlying age-induced skeletal muscle wasting: let's talk about sex

Alexandra Moreira-Pais<sup>a,b,c,\*</sup>, Rui Vitorino<sup>d</sup>, Cláudia Sousa-Mendes<sup>e</sup>, Maria João Neuparth<sup>a,f</sup>, Alessandro Nuccio<sup>b,g</sup>, Claudio Luparello<sup>g</sup>, Alessandro Attanzio<sup>g</sup>, Petr Novák<sup>h</sup>, Dmitry Loginov<sup>h</sup>, Rita Nogueira-Ferreira<sup>e</sup>, Adelino Leite-Moreira<sup>e,i</sup>, Paula A. Oliveira<sup>c</sup>, Rita Ferreira<sup>b</sup>, José A. Duarte<sup>f,j</sup>

<sup>a</sup> Research Center in Physical Activity, Health and Leisure (CIAFEL), Faculty of Sport, University of Porto (FADEUP) and Laboratory for Integrative and Translational Research in Population Health (ITR), 4200-450, Porto, Portugal

<sup>b</sup> LAQV-REQUIMTE, Department of Chemistry, University of Aveiro, 3810-193, Aveiro, Portugal

<sup>c</sup> Centre for Research and Technology of Agro Environmental and Biological Sciences (CITAB), Inov4Agro, University of Trás-os-Montes and Alto Douro (UTAD), Quinta de Prados, 5000-801, Vila Real, Portugal

<sup>d</sup> iBiMED - Institute of Biomedicine, Department of Medical Sciences, University of Aveiro, 3810-193, Aveiro, Portugal

<sup>e</sup> Cardiovascular R&D Center - UnIC@RISE, Department of Surgery and Physiology, Faculty of Medicine of the University of Porto, 4200-319, Porto, Portugal

<sup>f</sup> UCIBIO - Applied Molecular Biosciences Unit, Translational Toxicology Research Laboratory, University Institute of Health Sciences (IH-TOXRUN, IUCS-CESPU), 4585-116, Gandra, Portugal

<sup>g</sup> Department of Biological, Chemical and Pharmaceutical Sciences and Technologies (STEBICEF), University of Palermo, 90128, Palermo, Italy

<sup>h</sup> Laboratory of Structural Biology and Cell Signalling, Institute of Microbiology of the Czech Academy of Sciences, Prumyslova 595, CZ-252 50, Vestec, Czech Republic

<sup>i</sup> Department of Cardiothoracic Surgery, Centro Hospitalar Universitário São João, 4200-319, Porto, Portugal

<sup>j</sup> Associate Laboratory i4HB - Institute for Health and Bioeconomy, University Institute of Health Sciences - CESPU, 4585-116, Gandra, Portugal

### ARTICLE INFO

#### Keywords:

Fatty acid oxidation  
Mitophagy  
Oxidative phosphorylation  
Sarcopenia  
Sexual dimorphism

### ABSTRACT

Sarcopenia is associated with reduced quality of life and premature mortality. The sex disparities in the processes underlying sarcopenia pathogenesis, which include mitochondrial dysfunction, are ill-understood and can be decisive for the optimization of sarcopenia-related interventions. To improve the knowledge regarding the sex differences in skeletal muscle aging, the *gastrocnemius* muscle of young and old female and male rats was analyzed with a focus on mitochondrial remodeling through the proteome profiling of mitochondria-enriched fractions. To the best of our knowledge, this is the first study analyzing sex differences in skeletal muscle mitochondrial proteome remodeling. Data demonstrated that age induced skeletal muscle atrophy and fibrosis in both sexes. In females, however, this adverse skeletal muscle remodeling was more accentuated than in males and might be attributed to an age-related reduction of 17beta-estradiol signaling through its estrogen receptor alpha located in mitochondria. The females-specific mitochondrial remodeling encompassed increased abundance of proteins involved in fatty acid oxidation, decreased abundance of the complexes subunits, and enhanced proneness to oxidative posttranslational modifications. This conceivable accretion of damaged mitochondria in old females might be ascribed to low levels of Parkin, a key mediator of mitophagy. Despite skeletal muscle atrophy and fibrosis, males maintained their testosterone levels throughout aging, as well as their androgen receptor content, and the age-induced mitochondrial remodeling was limited to increased abundance of pyruvate dehydrogenase E1 component subunit beta and electron transfer flavoprotein subunit beta. Herein, for the first time, it was demonstrated that age affects more severely the skeletal muscle mitochondrial proteome of females, reinforcing the necessity of sex-personalized approaches towards sarcopenia management, and the inevitability of the assessment of mitochondrion-related therapeutics.

\* Corresponding author. Departamento de Química, Universidade de Aveiro, Campus Universitário de Santiago, 3810-193, Aveiro, Portugal.

E-mail addresses: [alexandrapais@ua.pt](mailto:alexandrapais@ua.pt) (A. Moreira-Pais), [rvitorino@ua.pt](mailto:rvitorino@ua.pt) (R. Vitorino), [csmdes@med.up.pt](mailto:csmdes@med.up.pt) (C. Sousa-Mendes), [mneuparth@hotmail.com](mailto:mneuparth@hotmail.com) (M.J. Neuparth), [alessandro.nuccio@community.unipa.it](mailto:alessandro.nuccio@community.unipa.it) (A. Nuccio), [claudio.luparello@unipa.it](mailto:claudio.luparello@unipa.it) (C. Luparello), [alessandro.attanzio@unipa.it](mailto:alessandro.attanzio@unipa.it) (A. Attanzio), [pnovak@biomed.cas.cz](mailto:pnovak@biomed.cas.cz) (P. Novák), [dmitry.loginov@biomed.cas.cz](mailto:dmitry.loginov@biomed.cas.cz) (D. Loginov), [rmferreira@med.up.pt](mailto:rmferreira@med.up.pt) (R. Nogueira-Ferreira), [amoreira@med.up.pt](mailto:amoreira@med.up.pt) (A. Leite-Moreira), [pamo@utad.pt](mailto:pamo@utad.pt) (P.A. Oliveira), [ritaferreira@ua.pt](mailto:ritaferreira@ua.pt) (R. Ferreira), [jose.duarte@iucs.cespu.pt](mailto:jose.duarte@iucs.cespu.pt) (J.A. Duarte).

<https://doi.org/10.1016/j.freeradbiomed.2024.04.005>

Received 20 February 2024; Received in revised form 31 March 2024; Accepted 1 April 2024

Available online 2 April 2024

0891-5849/© 2024 The Authors. Published by Elsevier Inc. This is an open access article under the CC BY-NC-ND license (<http://creativecommons.org/licenses/by-nc-nd/4.0/>).

## 1. Introduction

The world undergoes a sustained transformation in the age organization of the population driven by increasing life expectancy and decreasing fertility levels, with the global population aged 65 years or older being expected to increase from 9.3% in 2020 to 16.0% by 2050 [1]. This event is accompanied by diverse diseases namely sarcopenia, which is a muscle disease defined by low levels of muscle strength, muscle quantity or quality and physical performance that develops gradually throughout lifetime [2]. Sarcopenia is related to an increased risk of disability and consequent hospitalization, a higher hospital stay length, an increased risk of postoperative complications, frailty, mobility limitations, and premature mortality [3]. The pathogenesis of sarcopenia is multifactorial and may involve systemic changes like hormonal alterations and chronic inflammation, and local alterations such as neuromuscular junction (NMJ) degeneration, muscle fat infiltration, mitochondrial dysfunction, and oxidative stress [4]. Nonetheless, the precise role and contribution of each one of these processes to sarcopenia development and progression are not yet entirely recognized [5], making sarcopenia management challenging.

Mitochondrial dysfunction is advocated as a central factor associated with skeletal muscle aging with a growing body of evidence provided by both animal and human studies as elegantly reviewed by Bellanti and collaborators [6]. Besides energy production, the mitochondrion performs essential functions in skeletal muscle fibers, namely the regulation of intracellular calcium homeostasis and apoptotic signaling [4]. It is believed that the age-related decline of skeletal muscle quality is associated with a reprogramming of the skeletal muscle metabolism that results in an impaired uptake and utilization of glucose, fat and proteins, and a defective production of energy [6]. Aging also appears to induce a shift in the redox status towards oxidation, which is accompanied by overwhelmed or dysfunctional antioxidant defense mechanisms, ensuing an amplified susceptibility of cellular and subcellular environments to damage [7]. Along with mitochondrial remodeling, an age-related decrease in the levels of sex steroid hormones in both women and men has been proposed as an important driver of sarcopenia [8,9]. In fact, these hormones can modulate *via* their receptors distinct signaling pathways in skeletal muscle, but the precise outcomes and sex disparities are not completely acknowledged, principally in skeletal muscle aging [10]. In mitochondrion, this sex specificity seems to be also present, with the suggestion that old females have lower function of the oxidative phosphorylation (OXPHOS) complexes than old males [11, 12]. To date, the mechanisms behind the effect of sex on sarcopenia development and on age-related mitochondrial remodeling in the skeletal muscle are yet to be fully uncovered. Coupled with this gap are the equivocal data retrieved from clinical studies on the effect of sex on skeletal muscle remodeling, probably due to different selection criteria that can bias the results, such as physical status and comorbidities. In this regard, the use of preclinical models allows the control of not only physical activity but also nutritional status, both of which can influence the outcomes of the studies. The recognition of sex-specific players involved in age-related skeletal muscle impairment will enable the development of preventive and therapeutic interventions tailored to the sex of each patient towards improved chances of survival and quality of life.

Hence, the overarching goal of this study was to investigate the effect of sex on age-related skeletal muscle wasting with a focus on mitochondrial remodeling. Specifically, we examined the *per se* effect of sex and aging and their interplay on the *gastrocnemius* muscle mass, fiber cross-sectional area (CSA) and fibrosis, and its association with the circulating levels of sex hormones and the muscle content of their receptors. Mass-spectrometry (MS) profiling of mitochondria-enriched fractions was performed to uncover the age-induced skeletal muscle mitochondrial remodeling, comprising the identification of mitochondrial proteins more prone to posttranslational modifications (PTMs) that may contribute to the aging phenotype. The use of rats in this study was

a well thought-through choice based on the chronic nature of sarcopenia that takes years to develop in humans and the consequent extended time course and ethical concerns surrounding the invasive acquisition of skeletal muscle biopsies from potentially frail individuals and also from healthy ones. Rats were selected based on evidence reporting that the pattern of skeletal muscle impairment in the rat (vs. mice) seems to be more representative of the human [13]. The *gastrocnemius* muscle was elected because it is believed to be affected by aging, it is fundamental for lower limb activities [14], for comparative proposes with other studies [13,14] and its thickness was proposed as a muscle mass index for sarcopenia diagnosis [15].

## 2. Materials and methods

### 2.1. Animal protocol

Female and male Wistar rats were obtained from the Charles River Laboratories (FR) at four (young groups) or twelve (old groups) weeks. Before the initiation of the experiments, all rats were acclimatized to the handler and the experimental protocol for one week and then randomly distributed (three to four rats *per* cage; 1500U Eurostandard Type IV S cages, Tecniplast, Varese, IT) into the experimental groups: young female ( $n = 7$ ), old female ( $n = 13$ ), young male ( $n = 8$ ), and old male ( $n = 11$ ). The rats were housed at controlled temperature ( $22 \pm 2^\circ\text{C}$ ) and relative humidity ( $50 \pm 5\%$ ) with a 12:12 h light-dark cycle with *ad libitum* food (standard diet 4RF21, Mucedola, Milan, IT) and water access. To mimic young adult and middle-age humans, the rats from the young groups were sacrificed at 6 months old (corresponds to approximately 18 years in humans [16]) and the rats from the old groups at 19 months old (corresponds to approximately 45–50 years in humans [16]) by an intraperitoneal overdose of ketamine ( $75\text{ mg kg}^{-1}$ , Imalgene 1000, Merial SAS, Lyon, FR) and xylazine ( $10\text{ mg kg}^{-1}$ , Rompun 2%, Bayer, Kiel, DE) followed by exsanguination as indicated by the Federation of European Laboratory Animal Science Associations [17]. Blood was collected from the heart, and the two *gastrocnemius* muscles of each rat were collected and weighed (*vide infra* for sample-specific processing). The right and left tibiae were dissected to determine tibia length, which is an indicator of animal body size that is independent of alterations in muscle and fat masses [18]. All the procedures were approved by the University of Trás-os-Montes and Alto Douro Ethics Review Body ORBEA (Orgão Responsável pelo Bem-Estar e Ética Animal, reference 424-e-DCV-2016) and by the Portuguese Competent Authority DGAV (Direção Geral de Alimentação e Veterinária, license numbers 021326 and 004583), according to the European Guidelines, and following the Portuguese law (decree-law number 113/2013) on animal protection for scientific purposes.

### 2.2. Serum samples preparation and analyses

The blood collected from the heart during the necropsy was allowed to clot and then centrifuged at  $4^\circ\text{C}$  for 15 min at 3000 g. The obtained serum was stored at  $-80^\circ\text{C}$  for the biochemical analyses that follow.

The serum levels of cholesterol, triglycerides, fasting glucose, and lactate were measured on an AutoAnalyzer (PRESTIGE 24i, Cormay PZ, Diamond Diagnostics, MA, US). Enzyme-linked immunosorbent assays (ELISA) were performed to determine the serum levels of 17 $\beta$ estradiol ( $\beta$ -estradiol (ab108667, abcam, Cambridge, UK) and testosterone (E-39, InterMedical Diagnostics, Naples, IT).

### 2.3. Histological analyses of the *gastrocnemius* muscle

Half of one *gastrocnemius* muscle ( $n = 5$  *per* group) was fixed in 4% paraformaldehyde and embedded in paraffin to prepare paraffin blocks, which were sectioned ( $3\text{ }\mu\text{m}$  of thickness) using a microtome and mounted on silane-coated slides. After deparaffinization through incubation at  $60^\circ\text{C}$  for 30 min and with xylol for 10 min, the slides were

hydrated in 5-min incubations with decreasing concentrations of ethanol aqueous solutions (100%, 90% and 70%, v/v) and water. The slides were then stained with hematoxylin and eosin (H&E; Hematoxylin H and Eosin Y 1%, BioGnost, Zagreb, HR) or Sirius Red (Direct Red 80, Sigma Aldrich, Missouri, US) to analyze the CSA and fibrosis area, respectively. Skeletal muscle images were acquired with a microscope (Olympus XC30 Digital Color Camera, Olympus, Tokyo, JP) and analyzed at 400x (CSA) or 200x (fibrosis) magnification with Cell<sup>B</sup> (version 5.1.0.2640, Olympus Soft Imaging Solutions, Tokyo, JP) and Image Pro Plus (version 6.0) software.

#### 2.4. Preparation of gastrocnemius muscle homogenates and mitochondria-enriched fractions

Approximately 50 mg of the other half of the *gastrocnemius* muscle was homogenized with a Teflon® pestle in a motor-driven Potter-Elvehjem glass homogenizer at 0–4 °C in a lysis buffer (0.5 mM EGTA, 10 mM HEPES, NaOH pH 7.4, 0.1% Triton X-100, 1:1000 PMSF and 1:400 protease inhibitor cocktail (P8340, Sigma-Aldrich, Missouri, US)) in the proportion of 50 mg of muscle to 1 mL of lysis buffer. The protein content of the muscle homogenates (henceforward named “total homogenate”) was assessed using the commercial kit DC™ Protein Assay (Bio-Rad, CA, US), according to the manufacturer’s instructions and using bovine serum albumin (BSA) as standard. Then, the total homogenates were preserved at –80 °C for the biochemical analyses described in subsections 2.5 and 2.6.

The other *gastrocnemius* muscle was used for mitochondria isolation based on Padrão and collaborators [19] with modifications. For MS analyses pooled tissue samples were considered (n = 6 per group). Briefly, muscles were finely minced in isolation buffer (20 mM MOPS, 1 mM EGTA, KOH pH 7.5, 110 mM KCl, and 2 mM PMSF) and incubated in 0.25 mg mL<sup>–1</sup> of trypsin (Sigma-Aldrich, Missouri, US). After removing the supernatant, the muscles were suspended in isolation buffer with 0.1% fatty acid-free BSA and homogenized with a motor-driven Teflon® Potter-Elvehjem homogenizer, followed by a centrifugation at 1000 g for 5 min. The collected supernatant was centrifuged at 12500 g for 10 min, followed by pellet resuspension in washing medium (10 mM HEPES, KOH pH 7.4, 250 mM sucrose, and 1:1000 PMSF) and centrifuged at 12500 g for 10 min, followed by new pellet resuspension and centrifugation. Lastly, the obtained pellet, which contained the mitochondrial fraction, was resuspended in washing medium supplemented with 1:400 of protease inhibitor cocktail (P8340, Sigma-Aldrich, Missouri, US) and stored at –80 °C for the biochemical analyses described in subsections 2.5 and 2.6. Regarding the pooled samples, the described procedure was equally implemented, with the exception that the final pellet containing the mitochondrial fraction was resuspended in 10 mM HEPES, KOH pH 7.4 (without protease inhibitors) and stored at –80 °C for the biochemical analyses described in subsection 2.7. All the procedures were performed at 0–4 °C. The protein content of the mitochondria-enriched fractions was assessed using the commercial kit RC-DC™ Protein Assay (Bio-Rad, CA, US), according to the manufacturer’s instructions and using BSA as standard. The purity of the mitochondria-enriched fractions was evaluated by immunoblotting, as described in subsection 2.6, with the use of sarcoplasmic/endoplasmic reticulum calcium ATPase 2 (SERCA2) as a cytoplasmic marker and adenosine triphosphate subunit beta (ATPB) as a mitochondrial marker and based on the results (Fig. S1) the mitochondria-enriched fractions were analyzed.

#### 2.5. Enzymatic assays in total homogenates and mitochondria-enriched fractions

Citrate synthase (CS) activity was assessed in total homogenates based on the method described by Coore and collaborators [20]. Briefly, 5,5'-dithiobis-(2-nitrobenzoic acid) reacted with the thiol groups of coenzyme A, previously released by the reaction of acetyl-CoA with

oxaloacetate, which was spectrophotometrically measured at 412 nm (molar extinction coefficient of 13.6 mM<sup>–1</sup> cm<sup>–1</sup>). The activity of CS was expressed in  $\mu\text{mol per minute per milligram of gastrocnemius total protein}$ .

Lactate dehydrogenase (LDH) activity was evaluated in total homogenates according to Šimaga and collaborators [21]. Concisely, the reduction of pyruvate to lactate was followed spectrophotometrically by the measurement of the decrease in the absorbance of nicotinamide adenine dinucleotide (NADH), due to its oxidation, at 340 nm (molar extinction coefficient of NADH 6.21 mM<sup>–1</sup> cm<sup>–1</sup>). The specific activity of LDH was expressed in units per milligram of *gastrocnemius* total protein. One unit of enzyme activity was defined as the amount of enzyme that transforms 1  $\mu\text{mol}$  of substrate in 1 min at room temperature and pH 7.0.

Adenosine triphosphate (ATP) synthase activity was evaluated in mitochondria-enriched fractions according to Morin and collaborators [22]. Succinctly, the reaction of phosphate, previously produced by the hydrolysis of ATP, with ammonium molybdate resulted in the formation of a complex that was reduced in the presence of the reducing agent ferrous sulfate, originating a colored complex (molybdenum blue), which was spectrophotometrically measured at 610 nm. Potassium dihydrogen phosphate was used as standard. The activity of ATP synthase was expressed in  $\mu\text{mol per minute per milligram of gastrocnemius total protein}$ .

#### 2.6. Immunoblot analyses in total homogenates and mitochondria-enriched fractions

To determine the content of protein carbonyls in mitochondria-enriched fractions, the samples were derivatized before the immunoblot analyses, as previously described [19]. Briefly, a certain volume (V) of the mitochondria-enriched fraction correspondent to 20  $\mu\text{g}$  of protein was mixed with 1 V of SDS 12% and 2 V of 10 mM dinitrophenylhydrazine in 10% trifluoroacetic acid (TFA), followed by 30 min of dark incubation. After this, 1.5 V of a solution constituted by 30% of glycerol and 18% of  $\beta$ -mercaptoethanol in Tris 2 M was added. The derivatized samples were electrophoresed on a 12.5% SDS-PAGE gel according to Laemmli [23] and then blotted onto a nitrocellulose membrane (Amersham™, Protan®, GE Healthcare, Illinois, US) for 2 h at 200 mA. The immunodetection was made using an anti-dinitrophenol (DNP) antibody (*vide infra*).

Regarding the remaining Western blot analyses, equivalent volumes to 50  $\mu\text{g}$  of protein of total homogenate or mitochondria-enriched fraction were electrophoresed on a 12.5% SDS-PAGE gel according to Laemmli [23] and then blotted onto a nitrocellulose membrane (Amersham™, Protan®, GE Healthcare, Illinois, US) for 2 h at 200 mA. Protein loading was controlled by Ponceau S staining, since most of the housekeeping markers used can be affected by stressful stimuli in the skeletal muscle [24].

Nonspecific binding was blocked by the incubation of the membranes in a 5% (w/v) solution of non-fat dry milk in Tris-buffered saline (TBS) with Tween 20 (TBST) for 1 h at room temperature and with agitation. Then, each membrane was incubated with the corresponding primary antibody: anti-ATPB (ab14730), anti-6-phosphofructokinase muscle type (PFKM, ab154804), anti-estrogen receptor alpha (ER $\alpha$ , ab32063), anti-peroxisome proliferator-activated receptor gamma coactivator 1-alpha (PGC1 $\alpha$ , ab191838), anti-mitochondrial encoded ATP synthase membrane subunit 6 (MT-ATP6, ab192423), anti-mitochondrial encoded cytochrome B (MT-CYB, ab81215), and anti-SERCA2 (ab2861) from Abcam (Cambridge, UK); anti-estrogen-related receptor alpha (ERR $\alpha$ , 07–662), anti-androgen receptor (AR, 06–680), and anti-DNP (MAB2223) from Sigma-Aldrich (Missouri, US); anti-PTEN-induced kinase 1 (PINK1, sc517353), and anti-Parkin (sc-32282) from Santa Cruz Biotechnology (Texas, US); and anti-ubiquitin (AUB01) from Cytoskeleton Inc. (Colorado, US). This incubation was followed by three 10-min washes with TBST, incubation with the corresponding

secondary antibody (anti-rabbit (NA934V) or anti-mouse (NA931V) from GE Healthcare, Illinois, US) and new washes. Both primary and secondary antibodies were diluted 1:1000 in 5% (w/v) non-fat dry milk in TBST. The primary antibody was incubated overnight at 4 °C, and the secondary antibody during 2 h at room temperature and with agitation. Immunoreactive bands were detected with enhanced chemiluminescence reagents (Clarity Max, Bio-Rad, CA, US) according to the manufacturer's procedure. Images were acquired using ChemiDoc Imaging System (Bio-Rad, CA, US) and analyzed using Image Lab software (version 6.0.0., Bio-Rad, CA, US). The optical density (OD) values were expressed in arbitrary units.

## 2.7. LC-MS/MS of mitochondria-enriched fractions

Mitochondria-enriched fractions were incubated with 50 mM 4-ethylmorpholine buffer (pH 8.5) supplemented with 6 M guanidine-HCl and 15% acetonitrile (ACN) in the ratio 1:5 (v/v). After sonication for 30 s and incubation on ice for 30 min, the samples were centrifuged at 10000 g for 5 min and the supernatant was collected. Total protein concentration was measured using the commercial kit BCA Protein Assay (Thermo Fisher Scientific, Massachusetts, US). An aliquot containing 10 µg of total protein was diluted with 10 mM 4-ethylmorpholine (pH 8.5) to a final volume of 20 µL. Samples were reduced and alkylated by adding 10 mM Tris(2-carboxyethyl)phosphine and 30 mM 2-chloroacetamide, followed by incubation at 70 °C for 5 min. A two-step digestion was performed. Firstly, LysC (Promega, Wisconsin, US) was added to the samples in the ratio 1:10 and incubated at 37 °C for 1 h. Secondly, trypsin (Promega, Wisconsin, US) was added in the ratio 1:10 and incubated at 37 °C for 2 h. The digestion process was terminated by the addition of TFA to a final concentration of 0.5% (v/v).

For MS and MS/MS analyses, peptides were desalted using the StageTip approach [25] and dried in SpeedVac concentrator. Prior to the MS analyses, the samples were dissolved in 20 µL of 2% ACN and 0.1% formic acid.

LC-MS/MS analyses were performed by using Vanquish Neo UHPLC system (Thermo Fisher Scientific, Massachusetts, US) coupled with timsTOF SCP mass spectrometer equipped with Captive spray (Bruker Daltonics, Massachusetts, US). Spectra were collected in a positive data dependent acquisition mode. Peptides were trapped onto C18 trap column (PepMap Neo C18 5 µm, 300 µm × 5 mm, Thermo Scientific, Massachusetts, US) for 3 min and then eluted to C18 analytical column (DNV PepMap Neo 75 µm × 150 mm, 2 µm, Thermo Scientific, Massachusetts, US). Both columns were heated to 50 °C. Peptide separation was carried out using a linear gradient of 5%–35% ACN over 35 min at a flow rate of 350 nL/min. Standard proteomics PASEF method was applied for data acquisition. The scan range was set from 0.6 to 1.6 V s/cm<sup>2</sup> and ramp time was 100 ms. A total of 10 PASEF MS/MS scans were performed. Precursor ions selected for fragmentation were in the *m/z* range of 100–1700 with charge states ≥2+ and ≤6+. Active exclusion was enabled for 0.4 min to prevent repeated selection of the same precursor ions. The MS proteomics data have been deposited to the ProteomeXchange Consortium via the PRIDE [26] partner repository with the dataset identifier PXD048802.

Proteins were identified using MaxQuant software (version 1.6.5.0, Max Planck Institute of Biochemistry, Planegg, DE). MS data were analyzed for quantitative comparisons using the Perseus software (version 2.0.11.0, Max Planck Institute of Biochemistry, Planegg, DE). Principal component analysis (PCA) and partial least squares discriminant analysis (PLS-DA) were applied to examine proteome dynamics between groups (the raw data were log-transformed for these analyses). Volcano plots were used to annotate proteins that were present in significantly different amounts between groups. These analyses were performed using the MetaboAnalyst web portal (version 5.0, [www.metaboanalyst.ca](http://www.metaboanalyst.ca), accessed in July 2023). We also sought for specific PTMs that were searched in MaxQuant and then further confirmed by manual inspection of MS spectra. Oxidations at methionine (Met), histidine

(His), phenylalanine (Phe), tyrosine (Tyr) and tryptophan (Trp) were searched, given that these amino acids are generally most prone to oxidation due to the high reactivity of their side chains (e.g., sulfur-containing side chain and aromatic rings) towards various reactive oxygen species (ROS) [27]. Acetylation at lysine (Lys) was also searched since it is the most reported [28]. Only modifications with confidence levels higher than 95% and a false discovery rate (FDR) of 1% were considered.

## 2.8. Statistical analyses

Data normality was evaluated by the Shapiro-Wilk test, except for CSA data where the Kolmogorov-Smirnov test was employed. For immunoblotting, CSA and fibrosis data, the significant differences among groups were determined by performing the two-way analysis of variance (ANOVA) followed by Tukey's multiple comparisons post-hoc test, and the values are present as mean ± standard deviation (SD). When statistically significant, the results from the two-way ANOVA are given below the corresponding graphic or in the last column in the table. Pearson correlations were also performed, when considered relevant. *Gastrocnemius* muscle mass values were normalized to body weight and tibia length. These statistical analyses were performed using the GraphPad Prism software for Windows (version 6.01, California, US). For MS data, independent samples *t*-test analyses were employed in MetaboAnalyst web portal (version 5.0, [www.metaboanalyst.ca](http://www.metaboanalyst.ca), accessed in July 2023) to compare young female vs. old female, young male vs. old male, young female vs. young male and old female vs. old male. All the results were considered significantly different when *p* < 0.05.

## 3. Results

### 3.1. Characterization of the sex-specific systemic alterations and muscle morphological remodeling in response to aging

Table 1 shows that the body weight increased with age in both female and male rats with males having a higher body weight than females independently of age. To eliminate variations due to body weight changes with aging, the *gastrocnemius* muscle mass was normalized to body weight and a decrease in both old female and male rats was observed, indicative of age-related skeletal muscle wasting. To eliminate variations due to animal size changes with aging, the *gastrocnemius* muscle mass was normalized to tibia length and a sex-related increase of the ratio value in males compared to females was observed, which may be explained by the fact that male rats are usually larger than female rats due to a persistent difference in their growth curve [29].

To explore the effect of sex hormones on the age-induced skeletal muscle wasting observed, the serum levels of 17β-estradiol, which is the most potent estrogen that can also be produced by aromatization in the skeletal muscle [4], and testosterone were evaluated (Table 1). Old female rats had an approximately 79% decrease of the 17β-estradiol levels compared to young female rats and unchanged testosterone levels. No differences were observed in old male rats for either hormone.

Conventional biochemical analyses of serum samples were performed, where a typical aging phenotype [30] was observed with an age-induced increase of cholesterol and triglycerides levels in both sexes (Fig. S2). An age-induced increase in lactate serum levels was also present in both sexes (Fig. S2), which jointly with unchanged muscle PFKM levels and LDH activity with aging (Fig. S3) indicates an impaired lactate clearance due to, for instance, decreased hepatic gluconeogenesis or uptake into skeletal muscle, as suggested by the literature [31,32].

The observed age-induced loss of skeletal muscle mass in both sexes was allied to a decrease of the CSA of the *gastrocnemius* muscle fibers, which was higher in female rats (age-induced decrease of approximately 19% and 15% in, respectively, females and males; Fig. 1A). In accordance, old rats had a higher percentage of muscle fibers with inferior



Table 1

Anthropometric data given by body weight (BW), tibia length (TL), and *gastrocnemius* (GS) muscle mass in young female (n = 7), old female (n = 13), young male (n = 8), and old male (n = 11) rats. The *gastrocnemius* muscle mass normalized to body weight and tibia length is also depicted. The serum levels of 17β-estradiol and testosterone of young female (n = 5), old female (n = 10), young male (n = 5) and old male (n = 10) rats analyzed by ELISA are also displayed.

	Young Female	Old Female	Young Male	Old Male	% of total variation
BW (g)	278.71 ± 10.47****, #	405.93 ± 38.60	328.75 ± 20.24	638.64 ± 33.01****, #####	Interaction: 10.07, p<0.0001 Sex: 24.12, p<0.0001 Age: 57.66, p<0.0001
TL (cm)	3.6 ± 0.2****, #####	4.0 ± 0.1	4.3 ± 0.1	4.7 ± 0.1****, #####	Sex: 66.02, p<0.0001 Age: 20.94, p<0.0001
GS mass (g)	3.21 ± 0.21#####	3.30 ± 0.10	4.58 ± 0.31	5.23 ± 0.35****, #####	Interaction: 2.11, p<0.01 Sex: 73.97, p<0.0001 Age: 3.87, p<0.001
GS mass/BW (%)	1.15 ± 0.09****, #####	0.82 ± 0.07	1.40 ± 0.08	0.81 ± 0.04#####	Interaction: 6.26, p<0.0001 Sex: 5.35, p<0.0001 Age: 80.24, p<0.0001
GS mass/TL (g.cm <sup>-1</sup> %)	89.7 ± 3.1#####	83.1 ± 2.0	108.8 ± 6.1	111.9 ± 8.2****	Interaction: 2.71, p<0.05 Sex: 65.35, p<0.0001
17β-estradiol serum levels (pg. mL <sup>-1</sup> )	60.34 ± 1.74****, #####	12.55 ± 7.89	6.11 ± 2.88	11.06 ± 5.93	Interaction: 47.00, p<0.0001 Sex: 52.46, p<0.0001 Age: 31.00, p<0.0001
Testosterone serum levels (pg. mL <sup>-1</sup> )	0.06 ± 0.05	0.00(4) ± 0.00 (1)	2.13 ± 4.17	0.05 ± 0.01	

\*\*\*\*p<0.0001 vs. old female, \*\*\*p<0.001 vs. old female, #####p<0.0001 vs. young male, and #p<0.05 vs. young male.

CSA, varying from 676 to 5357 μm<sup>2</sup> and 793–7117 μm<sup>2</sup> in, respectively, old female and male rats compared to 1082–7510 μm<sup>2</sup> and 1372–6996 μm<sup>2</sup> in, respectively, young female and male rats (Fig. 1B). In contrast, old rats had increased fibrosis area, which was higher in females (approximately 3.4-fold and 3.0-fold age-induced increase in, respectively, females and males; Fig. 1C). In female rats, the fibers CSA was positively correlated with the serum levels of 17β-estradiol and testosterone, whereas the fibrosis area was negatively correlated with the serum levels of 17β-estradiol (Fig. 1F). For male animals, no correlation was found between histological findings and the circulating levels of sex hormones (Fig. S4).

3.2. Characterization of the sex-specific mitochondrial remodeling in response to aging

The assessment of the age-related mitochondrial remodeling was initiated by a general analysis in the total homogenate of common mitochondrial turnover-related proteins. The activity of CS was maintained throughout aging in both sexes but the levels of PGC1α increased

with age in females, which was accompanied by decreased Parkin levels (Fig. 2A).

Given the sex viewpoint of this study, the levels of ERα, ERRα (due to its possible contribution to mitochondrial function and skeletal muscle regeneration [33,34]) and AR were analyzed. Aging had no effect on the levels of these receptors when total homogenate was evaluated (Fig. 2A); however, aging affected the ERα mitochondrial pool of females, which was correlated with the decreased 17β-estradiol serum levels observed in these rats (Fig. 2B and C). In addition, mitochondrial density (given by CS activity) was positively correlated to whole muscle AR levels in both sexes, indicating that AR mitochondrial pool impacts whole muscle levels (Fig. 2C).

The mitochondrial proteome was then thoroughly explored by LC-MS/MS profiling of mitochondria-enriched fractions and consolidated with the analysis by immunoblotting of some specific protein markers performed in mitochondria-enriched fractions, as follow.

LC-MS/MS identified 445 distinct proteins with at least two unique peptides and a false discovery rate (FDR) of 1%. From these, 44% (196 proteins) were assigned as mitochondrial proteins according to MitoCarta3.0 [35]. However, data from *Rattus norvegicus* is not included in this inventory, and so, the comparison was made with data from *Mus musculus*. In addition, some of the identified proteins may be moonlighting proteins, thus having more than one location not yet validated and considered in MitoCarta3.0. Among the biological processes identified, the most predominant were maintenance of mitochondria location, metabolism, and regulation of skeletal muscle contraction. From the identified proteins, 364 were common to all groups, as demonstrated in the Venn diagram (Fig. S6).

Unsupervised PCA and supervised PLS-DA were performed to visualize group separation based on proteome datasets by means of dimensionality reduction. PCA analyses showed no clustering of proteome data *per* group (Fig. 3A), with a higher heterogeneity noticed in old male and young female rats. PLS-DA showed group separation being the age effect more prominent (Fig. 3B). To gain a better insight into the *per se* effect of sex and age, pairwise PCA and PLS-DA were performed. While PCA analyses showed no clustering of the proteome data, PLS-DA analyses demonstrated a similar separation between ages and between sexes, in an independent manner (Fig. 3C to J).

To identify proteins with statistically significant changes between groups, volcano plot analyses, which show log<sub>2</sub> of fold-change vs. log<sub>10</sub> of the *p*-value, were conducted, which resulted in the identification of 41 proteins (Fig. S7). Approximately 80.5% (33 proteins) of these proteins are localized in the mitochondrion of *Rattus norvegicus* (according to UniProt Knowledgebase (UniProtKB) [36] and Gene Ontology (GO)), and their details can be observed in Table 2. These proteins were included in a protein-protein interaction (PPI) analysis in STRING that demonstrated the interaction of trifunctional enzyme subunit beta (HADHB) with ERα and of CS with ERRα, whereas no interactions with AR were found (Fig. S8).

The mitochondrial proteome of females was more susceptible to age-related alterations, which will be briefly described. Increased amounts of HADHB, hydroxyacyl-coenzyme A dehydrogenase (HADH), enoyl-CoA delta isomerase (ECI1), and electron transfer flavoprotein subunit beta (ETFB) were observed, pointing towards an escalated fatty acid oxidation (FAO) in old female rats. Specific subunits of the OXPHOS complexes were also affected by aging in females, namely, decreased abundance of NADH dehydrogenase [ubiquinone] flavoprotein 2 (NDUFV2) from complex I, and increased and decreased abundance of, respectively, cytochrome *b*-c1 complex subunit 8 (UQCRCQ) and cytochrome *b*-c1 complex subunit 1 (UQCRC1) of complex III. Following these results, immunoblot analyses of mitochondrial deoxyribonucleic acid (mtDNA)-encoded proteins, which are essential for the function of the OXPHOS system, were performed (Fig. 4). While the levels of the subunit MT-ATP6 of ATP synthase were decreased in old female rats (vs. young females) and correlated with reduced ATP synthase activity, the levels of subunit MT-CYB of complex III were not modulated by age in

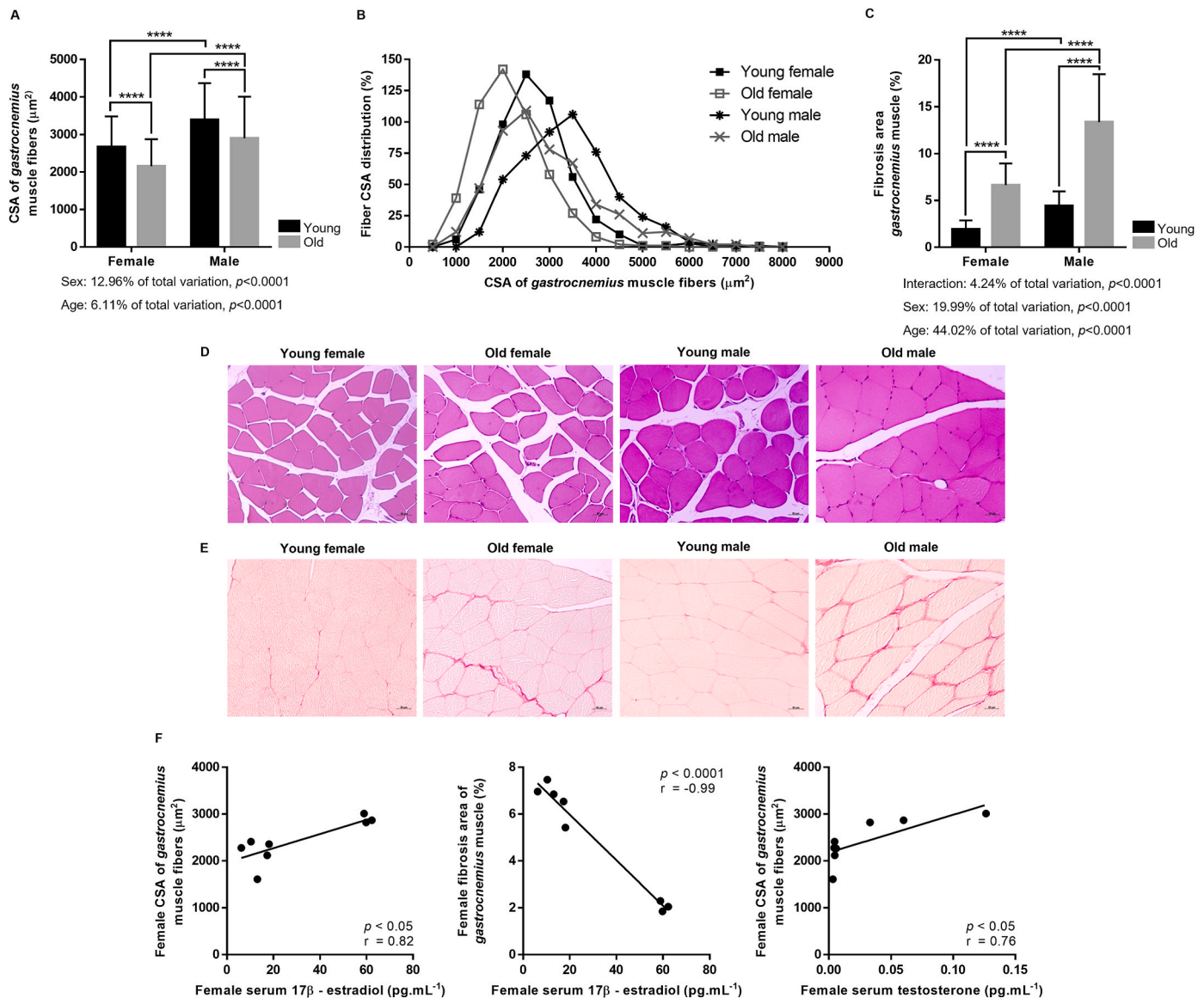


**Fig. 1.** (A) Cross-sectional area (CSA) of the *gastrocnemius* muscle fibers, (B) fiber CSA distribution of the *gastrocnemius* muscle, and (C) fibrosis area of the *gastrocnemius* muscle ( $n = 5$  per group in each analysis; \*\*\*\* $p < 0.0001$ ). Representative photomicrographs of (D) H&E-stained and (E) Sirius Red-stained *gastrocnemius* muscle sections. The bar scale represents 50  $\mu\text{m}$ . (F) Pearson correlations were performed for an in-deep understating of the results.

either sex.

Regarding males, the age-related alterations of the mitochondrial proteome were circumscribed to an increased abundance of pyruvate dehydrogenase E1 component subunit beta (PDHB) and ETFB.

The effect of sex at young and old ages was also noticed with, for instance, females having a higher abundance of proteins involved in tricarboxylic acid (TCA) cycle and amino acid catabolism at young age, and decreased abundance of proteins involved in ion transport at old age, compared to males. Of note, the abundance of phosphoglycerate kinase 1 (PGK1), which under stress stimuli translocates to the mitochondrion, was increased in old females compared to old males, which might have contributed to the increased lactate serum levels in old females (vs. old males) due to the PGK1-mediated inhibition of the pyruvate metabolism [37].

To further understand the effect of age and/or sex on mitochondrial proteome remodeling, we sought for specific PTMs. Table 3 lists the mitochondrial proteins identified as being more prone to oxidation and acetylation. Anew, the mitochondrial proteome of old female rats had a higher susceptibility to oxidation than the one of males. Indeed, only

ATP synthase subunit alpha (ATP5A1) was found oxidized at Met51 in old male rats. In old female rats, the proteins more prone to oxidation are involved in TCA cycle, including isocitrate dehydrogenase [NADP] (IDH2) and isocitrate dehydrogenase [NAD] subunit alpha (IDH3A) at, respectively, Met411 and Met206, and in OXPHOS, namely subunits ATP5A1 and ATP5MPL from ATP synthase at, respectively, Met189 and Met1. The higher susceptibility of OXPHOS proteins to oxidation is well known given the proximity of the complexes to mitochondria-generated ROS [38]. Some oxidative PTMs were found in both young and old female rats, but their levels were unchanged in response to aging. Malate dehydrogenase (MDH2), which is involved in TCA, was the only protein found to be acetylated. This PTM occurred at Lys307 in young female rats, and it is believed to enhance the enzyme activity by 3.9-fold without any other noteworthy reported effects [39].

Thenceforth the PTMs identified, ROS-induced carbonylation and the levels of total ubiquitination were examined by immunoblotting and no age-related alterations were noticed (Fig. 5). In addition, no differences were observed in the bands profile between groups in the DNP blot. Concerning the analysis of protein ubiquitination, only one band

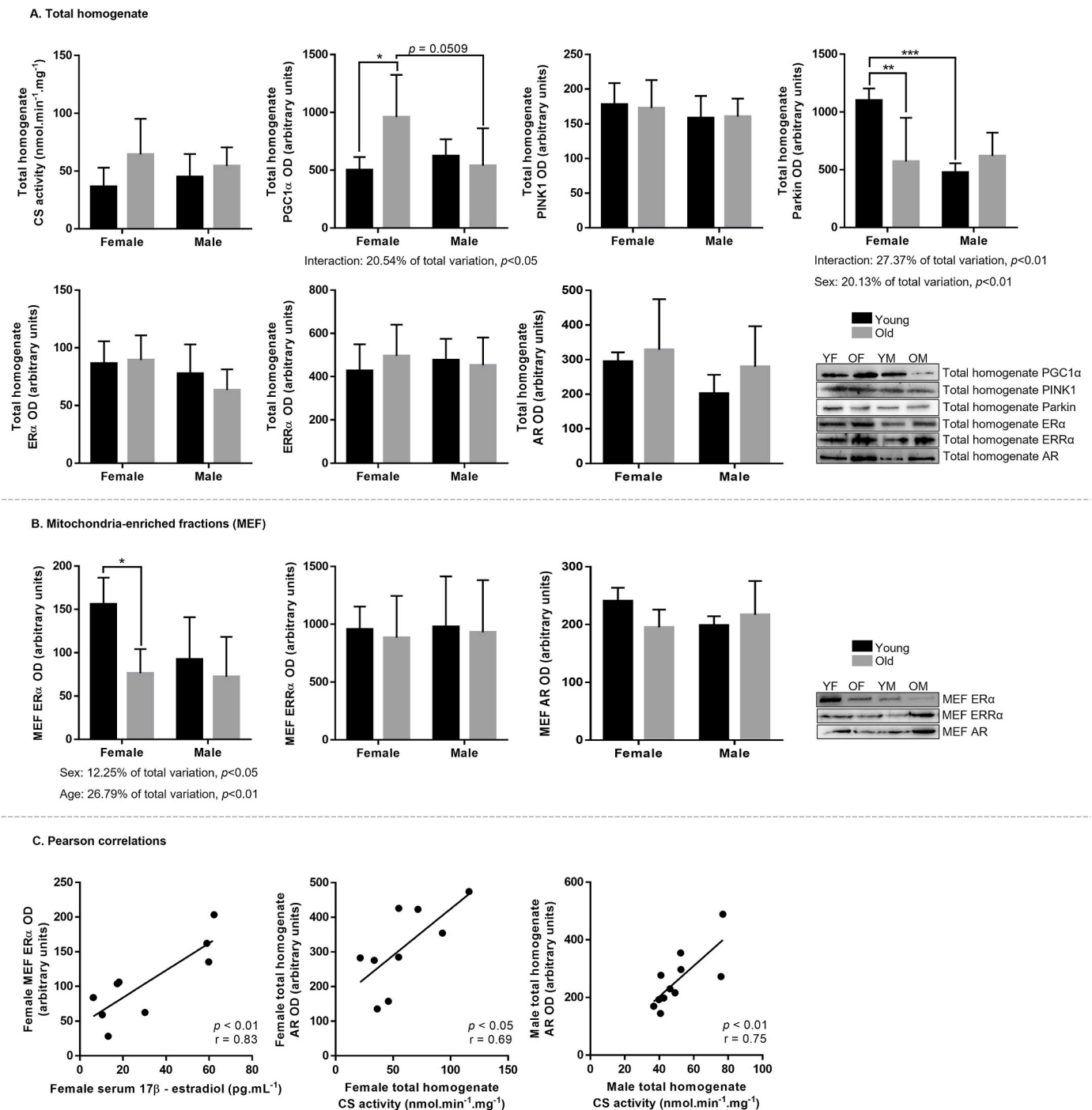


**Fig. 2.** The effect of aging and sex on the levels of PGC1α, PINK1, Parkin, ERα, ERRα and AR levels evaluated by immunoblotting in young female (YF), old female (OF), young male (YM) and old male (OM) rats in the (A) total homogenate (YF n = 6, OF n = 7, YM n = 7 and OM n = 7) or (B) mitochondria-enriched fractions (MEF; YF n = 6, OF n = 7, YM n = 6 and OM n = 7). (A) CS activity was spectrophotometrically evaluated in the total homogenate (YF n = 6, OF n = 7, YM n = 7 and OM n = 7). Representative immunoblot images are displayed. (C) Pearson correlations were performed for an in-deep understanding of the results (refer to Fig. S5 for non-significant correlations, \*\*\* $p < 0.001$ , \*\* $p < 0.01$ , and \*  $p < 0.05$ ).

between 50 and 75 kDa was detected in the blot, which may correspond to PINK1 or Parkin given their molecular weight, presence on mitochondria and known susceptibility to this PTM [40,41]. Ubiquitination of PINK1 ensures PINK1 homeostasis and function as a mitochondrial quality control factor [41] and ubiquitination of Parkin inhibits mitophagy [40]. The negative correlation between ubiquitinated and DNP-labeled proteins also indicates that low ubiquitin-dependent degradation contributes to the accretion of mitochondrial proteins damaged by carbonylation.

#### 4. Discussion

Data from the present study highlight the higher susceptibility of females to age-induced atrophy and fibrosis of the *gastrocnemius* muscle than males, which was associated with decreased 17β-estradiol levels. In agreement, the mitochondrial proteome of female rats was more prone to the effects of aging than the one of male rats and included a potential increase in FAO and impairment of OXPHOS function accompanied by a higher susceptibility to oxidative modifications. These data propose a

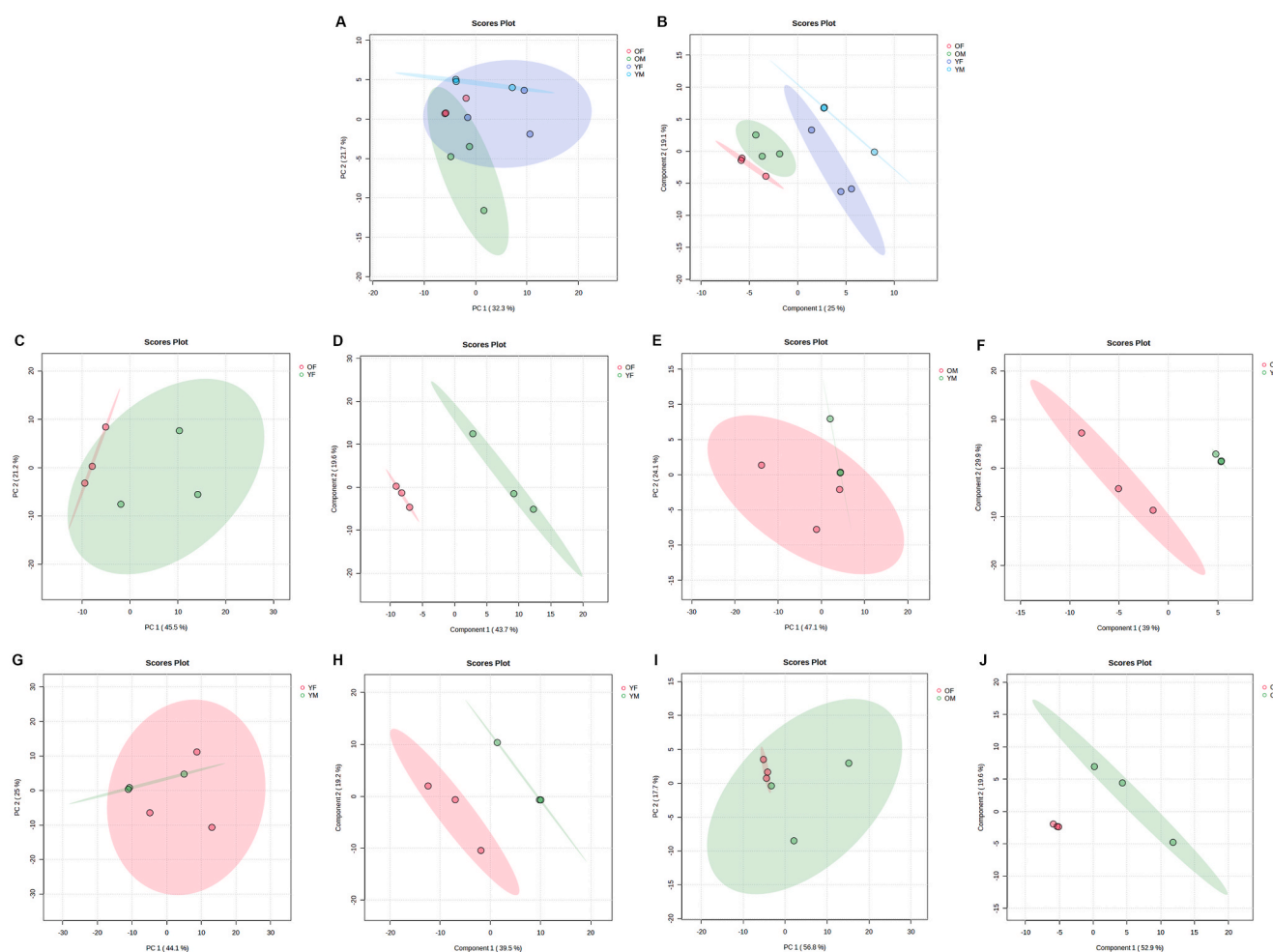


**Fig. 3.** (A, C, E, G, and I) PCA and (B, D, F, H, and J) PLS-DA analyses of the mitochondrial proteome data (YF, young female; OF, old female; YM, young male; OM, old male).

sex-specificity in the process of aging of the skeletal muscle mitochondrial proteome that may support sex disparities in age-related skeletal muscle wasting, which will be now dissected.

Both old female and male rats presented atrophy of the *gastrocnemius* muscle (Table 1), substantiated by decreased relative *gastrocnemius* muscle mass and fibers CSA, which was accompanied by an increased fibrosis (Fig. 1). Both histopathological modifications have been linked with impaired skeletal muscle functionality [42]. This adverse age-induced remodeling of the muscle was more accentuated in females, which was associated to their diminished 17 $\beta$ -estradiol serum levels (Fig. 1F; being 19 months old, these rats were expected to be in reproductive senescence, mimicking women menopause [43]). Low levels of this sex hormone may hamper skeletal muscle regeneration given its role in the activation and proliferation of satellite cells and in the down-regulation of inflammation (after muscle damage) and oxidative stress [44]. In agreement, the mitochondrial pool of ER $\alpha$  was reduced in old female rats (Fig. 2B) and its correlation with the decreased 17 $\beta$ -estradiol levels (Fig. 2C) insinuates an age-related dwindled signaling of this sex hormone through mitochondrial ER $\alpha$ . The idea of a modulation of mitochondrial functionality by this sex hormone was previously hypothesized [45]. In skeletal muscle, a diminished ER $\alpha$  signaling might impair mitophagy and mtDNA replication and increase the production of ROS [46]. Our findings substantiate an impaired mitophagy, evidenced by diminished levels of Parkin (Fig. 2A), and a decreased content of the ATP synthase subunit MT-ATP6 originated from mtDNA (Fig. 4), in the muscle of old females compared to their young counterparts.

Age-related skeletal muscle impairment is also vastly associated to reduced testosterone levels, particularly in men. Herein, testosterone levels, as well as AR levels, remained unchanged from young to old ages in male and female rats despite *gastrocnemius* muscle atrophy and fibrosis (Figs. 1, 2A and 2B). These results emphasize the magnitude of the non-generalization of the association between reduced skeletal muscle mass and strength and low testosterone levels [47], which can ensue the non-diagnosis of more than 80% of men that preserve normal levels throughout life [48]. To reinforce with a clinical viewpoint, sarcopenia was formerly diagnosed in older men with normal testosterone levels [49]. Still, in female rats, low testosterone levels seem to contribute to *gastrocnemius* muscle atrophy given the significant correlation observed (Fig. 1F).

Mitochondrial remodeling, the hub of this study, was initially perceived by the analysis of commonly analyzed markers of mitochondrial turnover. To start, age appeared to trigger mitochondrial biogenesis in female rats due to their elevated PGC1 $\alpha$  levels (Fig. 2A), which might reflect an endeavor to replace dysfunctional non-intact mitochondria, resulting in the unchanged CS activity observed. Nonetheless, an age-related decline in mitochondrial density due to a reduced biogenesis is pointed out by the literature [50].

Subsequently, the mitochondrial proteome was more exhaustively investigated by means of MS-based proteomics. The results revealed that females are more prone to age-induced mitochondrial alterations than males, with age simply increasing the abundance of PDHB and ETFB in male rats, vaguely suggesting an enhanced aerobic metabolism.



**Table 2**

List of mitochondrial proteins, identified by LC-MS/MS, whose abundance, given by the fold change ( $\log_2$ ), was significantly different ( $p < 0.05$ ) between groups in mitochondria-enriched fractions. Description of each protein including the accession number (AC) and the main biological process(es) are also present (according to UniProtKB database and GO for *Rattus norvegicus*).

AC UniProt	Protein name	Gene name	Fold change ( $\log_2$ )				Main biological process(es)
			OF vs. YF	OM vs. YM	YF vs. YM	OF vs. OM	
Q60587	Trifunctional enzyme subunit beta, mitochondrial	<i>Hadhb</i>	1.40			1.31	Fatty acid metabolism
Q9WVK7	Hydroxyacyl-coenzyme A dehydrogenase, mitochondrial	<i>Hadh</i>	1.21				Fatty acid metabolism
P23965	Enoyl-CoA delta isomerase 1, mitochondrial	<i>Eci1</i>	1.49				Fatty acid metabolism
Q704S8	Carnitine O-acetyltransferase	<i>Crat</i>			1.38		Fatty acid metabolism
P08461	Dihydrolipoyllysine-residue acetyltransferase component of pyruvate dehydrogenase complex, mitochondrial	<i>Dlat</i>	1.30				Carbohydrate/glucose metabolism
P49432	Pyruvate dehydrogenase E1 component subunit beta, mitochondrial	<i>Pdhb</i>		1.57		−0.81	Tricarboxylic acid cycle Carbohydrate/glucose metabolism
P16617	Phosphoglycerate kinase 1	<i>Pgk1</i>				1.57	Tricarboxylic acid cycle
Q01205	Dihydrolipoyllysine-residue succinyltransferase component of 2-oxoglutarate dehydrogenase complex, mitochondrial	<i>Dlst</i>				−0.87	Glucose metabolism Tricarboxylic acid cycle
P13086	Succinate-CoA ligase [ADP/GDP-forming] subunit alpha, mitochondrial	<i>Suc1g1</i>				1.69	Tricarboxylic acid cycle
P56574	Isocitrate dehydrogenase [NADP], mitochondrial	<i>Idh2</i>			0.98		Tricarboxylic acid cycle
Q8VHF5	Citrate synthase, mitochondrial	<i>Cs</i>			1.05		Tricarboxylic acid cycle
P10860	Glutamate dehydrogenase 1, mitochondrial	<i>Glud1</i>			1.14		Tricarboxylic acid cycle Regulation insulin secretion
P12007	Isovaleryl-CoA dehydrogenase, mitochondrial	<i>Ivd</i>			1.23		Glutamate catabolism
Q510C3	Methylcrotonoyl-CoA carboxylase subunit alpha, mitochondrial	<i>Mccc1</i>			1.49		Leucine catabolism
P07633	Propionyl-CoA carboxylase beta chain, mitochondrial	<i>Pccb</i>			1.58		Leucine catabolism Amino acid catabolism
P51650	Succinate-semialdehyde dehydrogenase, mitochondrial	<i>Aldh5a1</i>	1.21				Fatty acid catabolism Gamma-aminobutyric acid catabolism
Q02253	Methylmalonate-semialdehyde dehydrogenase [acylating], mitochondrial	<i>Aldh6a1</i>			2.13		Beta-alanine, thymine and valine catabolism
Q68FU3	Electron transfer flavoprotein subunit beta	<i>Etfb</i>	1.13	1.17			Electron transport
F7FFF0	Cytochrome b-c1 complex subunit 7	<i>LOC685596</i>	1.63				Electron transport
Q77Q16	Cytochrome b-c1 complex subunit 8	<i>Uqcqr</i>	1.31				Electron transport
Q68FY0	Cytochrome b-c1 complex subunit 1, mitochondrial	<i>Uqcrc1</i>	−1.00			−0.98	Electron transport
P19234	NADH dehydrogenase [ubiquinone] flavoprotein 2, mitochondrial	<i>Ndufv2</i>	−1.88				Electron transport
A9UMV9	NADH dehydrogenase [ubiquinone] 1 alpha subcomplex subunit 7	<i>Ndufa7l</i>	2.36			1.96	Electron transport
B2RZD6	NDUFA4, mitochondrial complex associated	<i>Ndufa4</i>	1.61		−1.22		Positive regulation of cytochrome c oxidase activity
P29418	ATP synthase subunit epsilon, mitochondrial	<i>Atp5e</i>	3.39				ATP synthesis
P85834	Elongation factor Tu, mitochondrial	<i>Tufm</i>				1.01	Protein biosynthesis
P16036	Solute carrier family 25 member 3	<i>Slc25a3</i>	−1.74				Phosphate ion transmembrane transport
F1LX07	Electrogenic aspartate/glutamate antiporter SLC25A12, mitochondrial	<i>Slc25a12</i>	−1.19				Aspartate and l-glutamate transmembrane transport
P81155	Voltage-dependent anion-selective channel protein 2	<i>Vdac2</i>				−0.83	Ion transport
Q9R1Z0	Voltage-dependent anion-selective channel protein 3	<i>Vdac3</i>				−1.80	Ion transport
P09605	Creatine kinase S-type, mitochondrial	<i>Ckmt2</i>				1.12	Phosphocreatine biosynthesis
A0A815ZLF3	AFG3 like matrix AAA peptidase subunit 2	<i>Afg3l2</i>	1.19				Proteolysis
P48721	Stress-70 protein, mitochondrial	<i>Hspa9</i>	1.18				Protein refolding
P26772	10 kDa heat shock protein, mitochondrial	<i>Hspe1</i>	1.05				Protein refolding

Abbreviations: OF, old female; YF, young female; OM, old male; YM, young male.

In contrast, categorical processes were found altered in old female rats, which will be now looked over. An age-induced escalated FAO was discerned in females that presented higher abundance of HADHB (also known as 3-ketoacyl-CoA thiolase, specific for long-chain fatty acid intermediates), HADH (also known as short-chain (S)-3-hydroxyacyl-CoA dehydrogenase, SCHAD, highly specific to short-chain fatty acid intermediates) and ECI1 (involved in the degradation of mono- and polyunsaturated fatty acids) (Table 2) [51]. It is worth noting that HADHB is believed to be negatively modulated by 17 $\beta$ -estradiol and tamoxifen (which can also function as an agonist) [52], possibly enlightening, at least in part, why HADHB levels were elevated in old female rats that had low 17 $\beta$ -estradiol levels. This age-related higher dependence on FAO of females may reflect the age-related remodeling of the muscle phenotype that comprises an increase in the number of slow-twitch fibers [53]. Data also uncovered a likely age-induced dysregulation of the

OXPHOS system in females noticed by, for example, the downregulation of the core subunit NDUFV2 from complex I as well of the subunit 1 (UQCRC1) from complex III, which was accompanied by an upregulation of subunits 7 (LOC685596) and 8 (UQCRCQ) also from complex III (Table 2). Since complexes I and III constitute the main sites of superoxide generation, their faulty function may ensue ROS production [54]. With regard to ATP synthase, an age-related increase in its subunit epsilon (ATP5E) was perceived in females (Table 2), as well as an age-related decrease in its mtDNA-encoded subunit 6 (MT-ATP6) that was correlated with low ATP synthase activity (Fig. 4), which can contribute to a weakened skeletal muscle contractility. Of note, most of disease-causing mutations in ATP synthase are located in the MT-ATP6 gene, reflecting the importance of this subunit in proton translocation, and have muscle weakness as one of the clinical manifestations [55]. The levels of MT-ATP6 appear to be positively modulated by

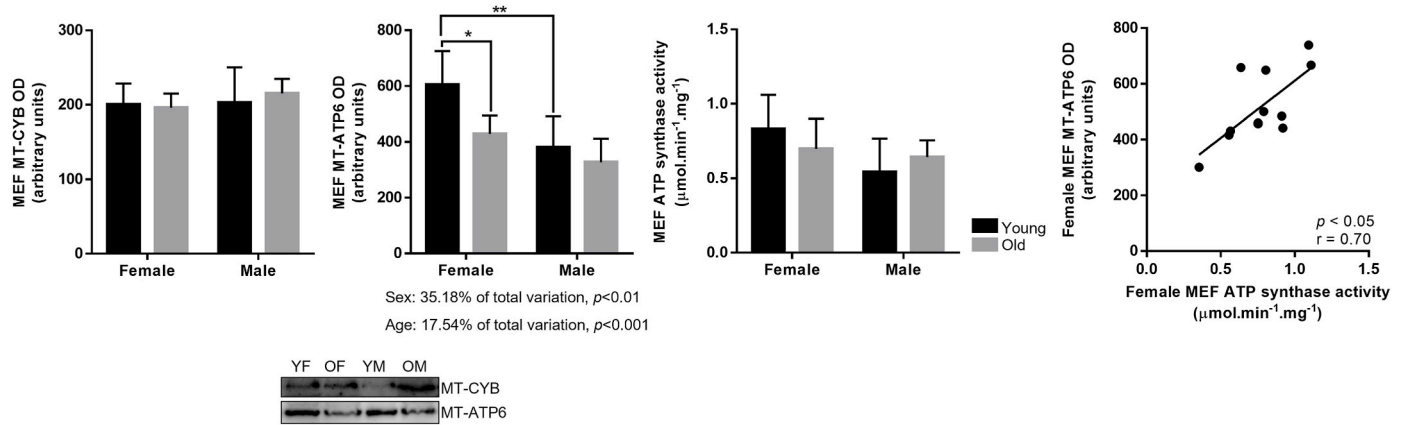


**Fig. 4.** The effect of aging and sex on the levels of MT-CYB and MT-ATP6 evaluated by immunoblotting, and in the activity of ATP synthase evaluated spectrophotometrically in mitochondria-enriched fractions (MEF) of young female (YF,  $n = 6$ ), old female (OF,  $n = 7$ ), young male (YM,  $n = 6$ ) and old male (OM,  $n = 7$ ) rats. Representative immunoblot images are displayed. Pearson correlations were performed for an in-deep understanding of the results. (refer to Fig. S9 for the non-significant correlation in males; \*\* $p < 0.01$  and \*  $p < 0.05$ ).

mitochondrial ER $\alpha$  given the correlation noticed (data not shown;  $p < 0.05$  and  $r = 0.71$ ), which is in line with previous findings [45]. Decreased abundance of solute carrier family 25 member 3 (SLC25A3, Table 2) might also contribute to a deficient OXPHOS-mediated ATP production in old female rats given its function in the transport of inorganic phosphate across the mitochondrial membrane for the final step of OXPHOS. As a matter of fact, reduced SLC25A3 levels were previously associated with muscle weakness, exercise intolerance and lactic acidosis (also noticed in old females), and the downregulation of SLC25A3 gene was reported in old sarcopenic women compared to old non-sarcopenic ones [56,57]. The decreased abundance of the electrogenic aspartate/glutamate antiporter SLC25A12 (SLC25A12) present in old females (Table 2) might also adversely influence ATP production due to its role in the malate-aspartate shuttle [58]. Its gene was found downregulated in the skeletal muscle of old women (vs. young women) [59], and gene mutations that cause reduced activity of the protein were associated with decreased ATP production [60].

The outcomes of age-related mitochondrial dysfunction ramify to an exacerbated production of ROS, primarily by the organelle itself, which can culminate in oxidative stress and severe damage to the cell, organelle membranes, DNA, lipids and proteins [61]. The evaluation of the susceptibility to oxidation, which is frequently a protein inactivating PTM [62], of skeletal muscle mitochondrial proteins revealed a higher proneness of the proteome of old females than the one of old males (Table 3), as suggested by the literature [63,64]. The opposite, however, was also reported [65]. Case in point, the subunits ATP5MPL and ATP5A1 of ATP synthase were found oxidized at, respectively, Met1 and Met189 in old females. The subunit ATP5A1 experienced dissimilar oxidations in all groups, but no significant differences between them were observed. Oxidation of the TCA cycle enzymes IDH2 and IDH3A at, respectively, Met411 and Met206 was also noticed in old females (Table 3), and IDH3A was previously found to be carbonylated in the *gastrocnemius* muscle of old female rats [66]. By being oxidatively modified, proteins can partially unfold, which is in line with the upregulation of the chaperones stress-70 protein (HSPA9) and 10 kDa heat shock protein (HSPE1), and of the protease AFG3 like matrix AAA peptidase subunit 2 (AFG3L2) in old females (Table 2). These proteins are involved in the mechanisms of protein quality control of mitochondria, namely the mitochondrial unfolded protein response (mtUPR), with the main aim of maintain proper folding and remove damaged proteins [67]. In the particular context of the data obtained in this study, the protease AFG3L2 may modulate MT-ATP6 processing, as previously reported [68], and the overexpression of PGC1 $\alpha$  was reported to stimulate the mtUPR in the form of an adaptative response of the skeletal muscle to acute exercise and in the context of Parkinson's

disease [69,70] in a non-sustained form. However, when persistently activated during adulthood, the mtUPR is believed to contribute to age-related muscle diseases like sarcopenia [71,72]. One alleged trigger of this activation is a defective mitophagy [71], which was implied to be present in old females given the reduced Parkin levels observed (Fig. 2A), since Parkin functions as a signal amplifier crucial for the assembly of ubiquitin chains on mitochondrion [73]. This low levels of Parkin in old females may vindicate the unchanged levels of ubiquitinated proteins in response to aging that, and in agreement with the negative correlation observed (Fig. 5), might contribute to the age-related accumulation of oxidatively modified mitochondrial proteins in female rats. Data concerning the age-related alterations in the content of ubiquitinated proteins is still open to questions given the higher or unchanged levels noticed in age-related studies as reviewed elsewhere [74]. A compromised mitophagy has been mentioned as one of the main culprits of the age-related accumulation of dysfunctional mitochondria, a famed hallmark of aging believed to be involved in skeletal muscle wasting and functional impairment [6,75–77].

Overall, this study endorses that the aging of the skeletal muscle and mitochondrion is sex-dependent. In females, the skeletal muscle was more affected by the age-induced remodeling of the mitochondrial proteome than in males. Specifically, in females occurred an age-related increase in the levels of proteins involved in FAO, decrease in the levels of subunits from complexes I, III and V, where low levels of the subunit MT-ATP6 were correlated with low ATP synthase activity, pointing towards an impaired ATP generation. In addition, a higher proneness to oxidative modifications of mitochondrial proteins involved in TCA and OXPHOS was observed in old females comparatively to old males. These specific age-induced effects in females were possibly prompted by an age-related decline in the levels of 17 $\beta$ -estradiol and of its receptor ER $\alpha$  in mitochondrion, highlighting a key role of 17 $\beta$ -estradiol signaling through mitochondrial ER $\alpha$ . This adverse females-specific remodeling probably contributed to their exacerbated skeletal muscle atrophy and fibrosis. The data from this study shed light on the significant role of sex disparities in skeletal muscle aging, particularly by underscoring that mitochondrion aging is a sex-specific process possibly modulated by mitochondrial ER $\alpha$  signaling. Importantly, this study strengthens the foundations of the urgent need of the inclusion of both sexes in skeletal muscle aging research to better understand the full spectrum of age-induced alterations and enable the sex-specific diagnostic and management of skeletal muscle diseases such as sarcopenia.

## Funding

A.M.-P. thanks the Portuguese Foundation for Science and

**Table 3**  
List of mitochondrial proteins more prone to oxidation or acetylation in mitochondria-enriched fractions, including their accession number (AC). The amino acid (AA) and the position of the modification (PM) are depicted. The group(s) where the modification was found is(are) also shown and, when possible, the comparison of the abundance between groups. The main biological process(es) of each protein is(are) described (according to UniProtKB database and GO for *Rattus norvegicus*).

AC Uniprot	Protein name	Gene name	AA	PM	Sequence	Identified in	OF vs. YF	YF vs. YM	Main biological process(es)
OXIDATION									
P56574	Isocitrate dehydrogenase [NADP], mitochondrial	<i>Idh2</i>	M	411	QTLEKVCVQTVESGAMTKDLAGCIHGLSNVK	OF			Tricarboxylic acid cycle
P56574	Isocitrate dehydrogenase [NADP], mitochondrial	<i>Idh2</i>	M	293	FDKNKIWYEHRLIDDMVAQVLKSSGGFVWAC	YF			Tricarboxylic acid cycle
Q99NA5	Isocitrate dehydrogenase [NAD] subunit alpha, mitochondrial	<i>Idh3a</i>	M	206	HRSNVTAVHKANIMRMSDGLFLQKCREVAEN	OF			Tricarboxylic acid cycle
P04636	Malate dehydrogenase, mitochondrial	<i>Mdh2</i>	M	266	MAYAGARFVFSLVDAMNGKEGVIECSFVQSK	YM			Tricarboxylic acid cycle
P21913	Succinate dehydrogenase [ubiquinone] iron-sulfur subunit, mitochondrial	<i>Sdhb</i>	M	73	PRMQTYKVDLNKCGPMVLDAIKIKNEIDST	YF YM		=	Tricarboxylic acid cycle
D3ZS58	NADH dehydrogenase [ubiquinone] 1 alpha subcomplex subunit 2	<i>Ndufa2</i>	M	89	NVSLNNLSAAEVTKAMENVLSGKA	OF YM			Electron transport Electron transport
P32551	Cytochrome <i>b</i> -c1 complex subunit 2, mitochondrial	<i>Uqcrc2</i>	M	217	EELHYFVQNHTSARMALVGLGVSHSILKEV	YF			Electron transport
P32551	Cytochrome <i>b</i> -c1 complex subunit 2, mitochondrial	<i>Uqcrc2</i>	M	437	DVVKAAKKFVSGKKSMTASGNLGHPTFLDEL	YM			Electron transport
P11240	Cytochrome <i>c</i> oxidase subunit 5 A, mitochondrial	<i>Cox5a</i>	M	70	YFNKPIDAWELRKGMNTLVGYDLVPEPKII	OF YF YM	=	=	Electron transport
P12075	Cytochrome <i>c</i> oxidase subunit 5 B, mitochondrial	<i>Cox5b</i>	M	64	REIMIAAQRLDPYNMLPPKAASGTKEDPNL	YM			Electron transport
P11951	Cytochrome <i>c</i> oxidase subunit 6C-2	<i>Cox6c2</i>	M	12	MSSGALLPKPQMRGLLAKRLRVHIVGA	OF YM			Electron transport
P35171	Cytochrome <i>c</i> oxidase subunit 7A2, mitochondrial	<i>Cox7a2</i>	M	41	NKVPEKQKLFQEDNGMPVHLKGGTSDALLYR	YF			Electron transport
A0A8I6AES7	NADH dehydrogenase [ubiquinone] iron-sulfur protein 7, mitochondrial	<i>Ndufs7</i>	F	115	HMAAPRYDMDRFGVVFRASPRQADVMIVAGT	YM			Electron transport
P15999	ATP synthase subunit alpha, mitochondrial	<i>Atp5a1</i>	M	189	LKAPGIIPRISVREPMQTGIKAVDLSLPIGR	OF			ATP synthesis
P15999	ATP synthase subunit alpha, mitochondrial	<i>Atp5a1</i>	M	324	IIYDDLKQAVAYRQMSLLRRPPGREAYPG	YF			ATP synthesis
P15999	ATP synthase subunit alpha, mitochondrial	<i>Atp5a1</i>	M	51	LHASNTRLQKTGTAE MSSILEERILGADTSV	OM YF			ATP synthesis
P15999	ATP synthase subunit alpha, mitochondrial	<i>Atp5a1</i>	Y	311	MGEYFRDNGKHALIYDDLKQAVAYRQMSL	YF YM	=		ATP synthesis
P10719	ATP synthase subunit beta, mitochondrial	<i>Atp5b</i>	M	145	APIKIPVGPETLGRIMNVIGEPIDERGPIKT	OF YF YM	=	=	ATP synthesis
P10719	ATP synthase subunit beta, mitochondrial	<i>Atp5b</i>	M	408	GIYPAVDPLDSTSRIIDPNIVGSEHYDVARG	YF YM		=	ATP synthesis
P10719	ATP synthase subunit beta, mitochondrial	<i>Atp5b</i>	M	113	EVAQHLGESTVRTIAMDGTEGLVRGQKVLD	YF YM		=	ATP synthesis
D3Z9R8	ATP synthase subunit ATP5MPL, mitochondrial	<i>Atp5mpl</i>	M	1	MLQSFIIKVVVWPMKPY	OF			ATP synthesis
Q6P9Y4	ADP/ATP translocase	<i>Slc25a4</i>	W	275	KIARDEGGKAFFKGAWSNVLRGMGGAFVLVL	OF			ADP/ATP transmembrane transport
P09605	Creatine kinase S-type, mitochondrial	<i>Ckmt2</i>	M	64	PPSADYPDLRKHNNCMAECLTPTTIYAKLRNK	YM			Phosphocreatine biosynthesis
P09605	Creatine kinase S-type, mitochondrial	<i>Ckmt2</i>	M	213	GLKGLAGRYYKLSEMTEQDQQLIDHFLF	YM			Phosphocreatine biosynthesis
ACETYLATION									
P04636	Malate dehydrogenase, mitochondrial	<i>Mdh2</i>	K	307	LLGKKGLEKNLIGIGKITPFEEKMIAEAIPE	YF			Tricarboxylic acid cycle

Abbreviations: YF, young female; OF, old female; YM, young male; OM, old male; M, methionine; F, phenylalanine; Y, tyrosine; W, tryptophane; K, lysine.

Technology (FCT)/Ministry of Science, Technology and Higher Education (MCTES) and the European Social Fund (ESF) through PT2020 for her grant (SFRH/BD/144396/2019). R.N.-F. acknowledges FCT for the research contract CEECIND/03935/2021 (<https://doi.org/10.54499/2021.03935.CEECIND/CP1685/CT0001>) under the CEEC Individual 2021.

Data availability statement

The data that support the findings of this study are available from the corresponding author upon reasonable request. Some data may not be made available because of privacy or ethical restrictions.

CRediT authorship contribution statement

Alexandra Moreira-Pais: Writing – original draft, Visualization,

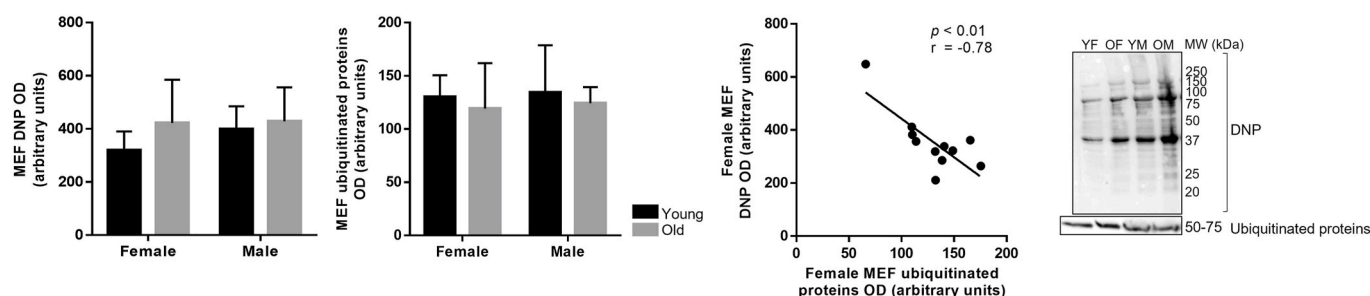


**Fig. 5.** The effect of aging and sex on the levels of DNP and ubiquitinated proteins in young female (YF,  $n = 6$ ), old female (OF,  $n = 7$ ), young male (YM,  $n = 6$ ) and old male (OM,  $n = 7$ ) rats, evaluated in mitochondria-enriched fractions (MEF) by immunoblotting. Representative immunoblot images are displayed along with the molecular weight (MW). Pearson correlations were performed for an in-deep understanding of the results (refer to Fig. S10 for the non-significant correlation in males).

Validation, Methodology, Investigation, Formal analysis. **Rui Vitorino:** Validation, Methodology, Formal analysis. **Cláudia Sousa-Mendes:** Methodology, Investigation. **Maria João Neuparth:** Investigation. **Alessandro Nuccio:** Investigation. **Claudio Luparello:** Writing – review & editing. **Alessandro Attanzio:** Writing – review & editing. **Petr Novák:** Methodology, Investigation. **Dmitry Loginov:** Methodology, Investigation. **Rita Nogueira-Ferreira:** Investigation. **Adelino Leite-Moreira:** Writing – review & editing. **Paula A. Oliveira:** Writing – review & editing, Supervision, Methodology. **Rita Ferreira:** Writing – review & editing, Visualization, Supervision, Formal analysis, Conceptualization. **José A. Duarte:** Writing – review & editing, Validation, Supervision, Conceptualization.

#### Declaration of competing interest

The authors declare that they have no known competing financial interests or personal relationships that could have appeared to influence the work reported in this paper.

#### Acknowledgments

This work was supported by CIAFEL (UIDB/00617/2020), ITR (LA/P/0064/2020), LAQV (UIDB/50006/2020), CITAB (UIDB/04033/2020, <https://doi.org/10.54499/UIDB/04033/2020>), UnIC (UIDB/IC/00051/2020 and UIDP/00051/2020), and RISE (LA/P/0053/2020) research units projects through national funds by the Portuguese Foundation for Science and Technology (FCT)/Ministry of Science, Technology and Higher Education (MCTES), by EPIC-XS (project number 0000475) funded by the Horizon 2020 program of the European Union, by Talking microbes - understanding microbial interactions within One Health framework (CZ.02.01.01/00/22\_008/0004597), by the Ministry of Education of the Czech Republic (Structural mass spectrometry CF - LM2018127 CIISB), and by the research project 2022.04344.PTDC (SEXDIFEND; <https://doi.org/10.54499/2022.04344.PTDC>).

#### Appendix A. Supplementary data

Supplementary data to this article can be found online at <https://doi.org/10.1016/j.freeradbiomed.2024.04.005>.

#### References

- [1] P.D. United Nations Department of Economic and Social Affairs, World Population Ageing 2020 Highlights: Living Arrangements of Older Persons, 2020.
- [2] A.J. Cruz-Jentoft, G. Bahat, J. Bauer, Y. Boirie, O. Bruyère, T. Cederholm, C. Cooper, F. Landi, Y. Rolland, A.A. Sayer, S.M. Schneider, C.C. Sieber, E. Topinkova, M. Vandewoude, M. Visser, M. Zamboni, W.G. for the E.W.G. on S. in O.P. (EWGOSOP2), E.G. for EWGOSOP2, Sarcopenia: revised european consensus on definition and diagnosis, *Age Ageing* 48 (2019) 16–31, <https://doi.org/10.1093/ageing/afy169>.
- [3] G. Coletta, S.M. Phillips, An elusive consensus definition of sarcopenia impedes research and clinical treatment: a narrative review, *Ageing Res. Rev.* 86 (2023) 101883, <https://doi.org/10.1016/j.arr.2023.101883>.
- [4] X. Tian, S. Lou, R. Shi, From mitochondria to sarcopenia: role of 17 $\beta$ -estradiol and testosterone, *Front. Endocrinol.* 14 (2023) 1156583, <https://doi.org/10.3389/fendo.2023.1156583>.
- [5] F. Petermann-Rocha, V. Balntzi, S.R. Gray, J. Lara, F.K. Ho, J.P. Pell, C. Celis-Morales, Global prevalence of sarcopenia and severe sarcopenia: a systematic review and meta-analysis, *J. Cachexia. Sarcopenia Muscle* 13 (2022) 86–99, <https://doi.org/10.1002/jcsm.12783>.
- [6] F. Bellanti, A. Lo Buglio, G. Vendemiale, Mitochondrial impairment in sarcopenia, *Biology* 10 (2021) 31, <https://doi.org/10.3390/biology10010031>.
- [7] E. Ferri, E. Marzetti, R. Calvani, A. Picca, M. Cesari, B. Arosio, Role of age-related mitochondrial dysfunction in sarcopenia, *Int. J. Mol. Sci.* 21 (2020) 5236, <https://doi.org/10.3390/ijms21155236>.
- [8] K. Shigehara, Y. Kato, K. Izumi, A. Mizokami, Relationship between testosterone and sarcopenia in older-adult men: a narrative review, *J. Clin. Med.* 11 (2022) 6202, <https://doi.org/10.3390/jcm11206202>.
- [9] A. Geraci, R. Calvani, E. Ferri, E. Marzetti, B. Arosio, M. Cesari, Sarcopenia and menopause: the role of estradiol, *Front. Endocrinol.* 12 (2021) 682012, <https://doi.org/10.3389/fendo.2021.682012>.
- [10] Y.J. Kim, A. Tamadon, H.T. Park, H. Kim, S.-Y. Ku, The role of sex steroid hormones in the pathophysiology and treatment of sarcopenia, *Osteoporos. Sarcopenia.* 2 (2016) 140–155, <https://doi.org/10.1016/j.afos.2016.06.002>.
- [11] P.A. Kramer, P.M. Coen, P.M. Cawthon, G. Distefano, S.R. Cummings, B. H. Goodpaster, R.T. Hepple, S.B. Kritchevsky, E.G. Shankland, D.J. Marcinek, F.G. S. Toledo, K.A. Duchowny, S. V Ramos, S. Harrison, A.B. Newman, A.J.A. Molina, Skeletal muscle energetics explain the sex disparity in mobility impairment in the Study of Muscle, Mobility and Aging (SOMMA), *Journals Gerontol. Ser. A.* (2023) glad283, <https://doi.org/10.1093/gerona/glad283>.
- [12] M. Triolo, A.N. Oliveira, R. Kumari, D.A. Hood, The influence of age, sex, and exercise on autophagy, mitophagy, and lysosome biogenesis in skeletal muscle, *Skelet. Muscle* 12 (2022) 1–18, <https://doi.org/10.1186/s13395-022-00296-7>.
- [13] A. Börsch, D.J. Ham, N. Mittal, L.A. Tintignac, E. Migliavacca, J.N. Feige, M. A. Rüegg, M. Zavalan, Molecular and phenotypic analysis of rodent models reveals conserved and species-specific modulators of human sarcopenia, *Commun. Biol.* 4 (2021) 194, <https://doi.org/10.1038/s42003-021-01723-z>.
- [14] W. Xie, M. He, D. Yu, Y. Wu, X. Wang, S. Lv, W. Xiao, Y. Li, Mouse models of sarcopenia: classification and evaluation, *J. Cachexia. Sarcopenia Muscle.* 12 (2021) 538–554, <https://doi.org/10.1002/jcsm.12709>.
- [15] S. Yaguchi, R. Asahi, T. Kamo, M. Azami, H. Ogihara, Prediction model including gastrocnemius thickness for the skeletal muscle mass index in Japanese older adults, *Int. J. Environ. Res. Publ. Health* 19 (2022) 4042, <https://doi.org/10.3390/ijerph19074042>.
- [16] P. Sengupta, The laboratory rat: relating its age with human's, *Int. J. Prev. Med.* 4 (2013) 624–630.
- [17] D. Forbes, H. Blom, N. Kostomitsopoulos, G. Moore, G. Perretta, Euroguide on the Accommodation and Care of Animals Used for Experimental and Other Scientific Purposes, 2007. London.
- [18] F.C. Yin, H.A. Spurgeon, K. Rakusan, M.L. Weisfeldt, E.G. Lakatta, Use of tibial length to quantify cardiac hypertrophy: application in the aging rat, *Am. J. Physiol.* 243 (1982) H941–H947, <https://doi.org/10.1152/ajpheart.1982.243.6.h941>.
- [19] A.I. Padrão, R. Ferreira, R. Vitorino, R.M.P. Alves, P. Figueiredo, J.A. Duarte, F. Amado, Effect of lifestyle on age-related mitochondrial protein oxidation in mice cardiac muscle, *Eur. J. Appl. Physiol.* 112 (2012) 1467–1474, <https://doi.org/10.1007/s00421-011-2100-3>.
- [20] H.G. Coore, R.M. Denton, B.R. Martin, P.J. Randle, Regulation of adipose tissue pyruvate dehydrogenase by insulin and other hormones, *Biochem. J.* 125 (1971) 115–127, <https://doi.org/10.1042/bj1250115>.
- [21] S. Šimaga, M. Abramčić, M. Osmak, D. Babić, J. Ilić-Forko, Total tissue lactate dehydrogenase activity in endometrial carcinoma, *Int. J. Gynecol. Cancer* 18 (2008) 1272–1278, <https://doi.org/10.1111/j.1525-1438.2008.01196.x>.
- [22] C. Morin, R. Zini, N. Simon, P. Charbonnier, J.-P. Tillement, H. Le Louet, Low glucocorticoid concentrations decrease oxidative phosphorylation of isolated rat brain mitochondria: an additional effect of dexamethasone, *Fundam. Clin.*



- Pharmacol. 14 (2000) 493–500, <https://doi.org/10.1111/j.1472-8206.2000.tb00432.x>.
- [23] U.K. Laemmli, Cleavage of structural proteins during the assembly of the head of bacteriophage T4, *Nature* 227 (1970) 680–685, <https://doi.org/10.1038/227680a0>.
- [24] A. Vigelsø, R. Dybbøe, C.N. Hansen, F. Dela, J.W. Helge, A.G. Grau, GAPDH and  $\beta$ -actin protein decreases with aging, making Stain-Free technology a superior loading control in Western blotting of human skeletal muscle, *J. Appl. Physiol.* 118 (2015) 386–394, <https://doi.org/10.1152/japplphysiol.00840.2014>.
- [25] J. Rappsilber, M. Mann, Y. Ishihama, Protocol for micro-purification, enrichment, pre-fractionation and storage of peptides for proteomics using StageTips, *Nat. Protoc.* 2 (2007) 1896–1906, <https://doi.org/10.1038/nprot.2007.261>.
- [26] Y. Perez-Riverol, J. Bai, C. Bandla, D. García-Seisdedos, S. Hewapathirana, S. Kamatchinathan, D.J. Kundu, A. Prakash, A. Frericks-Zipper, M. Eisenacher, M. Walzer, S. Wang, A. Brazma, J.A. Vizcaíno, The PRIDE database resources in 2022: a hub for mass spectrometry-based proteomics evidences, *Nucleic Acids Res.* 50 (2022) D543–D552, <https://doi.org/10.1093/nar/gkab1038>.
- [27] L. Grassi, C. Cabrele, Susceptibility of protein therapeutics to spontaneous chemical modifications by oxidation, cyclization, and elimination reactions, *Amino Acids* 51 (2019) 1409–1431, <https://doi.org/10.1007/s00726-019-02787-2>.
- [28] S. Ramazi, J. Zahiri, Post-translational modifications in proteins: resources, tools and prediction methods, *Database* 2021 (2021) baab012, <https://doi.org/10.1093/database/baab012>.
- [29] A.K. Slob, J.J. van der Werff Ten Bosch, Sex differences in body growth in the rat, *Physiol. Behav.* 14 (1975) 353–361, [https://doi.org/10.1016/0031-9384\(75\)90044-X](https://doi.org/10.1016/0031-9384(75)90044-X).
- [30] H.-H. Liu, J.-J. Li, Aging and dyslipidemia: a review of potential mechanisms, *Ageing Res. Rev.* 19 (2015) 43–52, <https://doi.org/10.1016/j.arr.2014.12.001>.
- [31] S. Masuda, T. Hayashi, T. Egawa, S. Taguchi, Evidence for differential regulation of lactate metabolic properties in aged and unloaded rat skeletal muscle, *Exp. Gerontol.* 44 (2009) 280–288, <https://doi.org/10.1016/j.exger.2008.12.003>.
- [32] D.B. Horn, D.A. Podolin, J.E. Friedman, D.A. Scholnick, R.S. Mazzeo, Alterations in key gluconeogenic regulators with age and endurance training, *Metabolism* 46 (1997) 414–419, [https://doi.org/10.1016/S0026-0495\(97\)90058-5](https://doi.org/10.1016/S0026-0495(97)90058-5).
- [33] K. Yoh, K. Ikeda, K. Horie, S. Inoue, Roles of estrogen, estrogen receptors, and estrogen-related receptors in skeletal muscle: regulation of mitochondrial function, *Int. J. Mol. Sci.* 24 (2023) 1853, <https://doi.org/10.3390/ijms24031853>.
- [34] I. Casaburi, A. Chimento, A. De Luca, M. Nocito, S. Sculco, P. Avena, F. Trotta, V. Rago, R. Sirianni, V. Pezzi, Cholesterol as an endogenous ER $\alpha$  agonist: a new perspective to cancer treatment, *Front. Endocrinol.* 9 (2018) 525, <https://doi.org/10.3389/fendo.2018.00525>.
- [35] S. Rath, R. Sharma, R. Gupta, T. Ast, C. Chan, T.J. Durham, R.P. Goodman, Z. Grabarek, M.E. Haas, W.H.W. Hung, P.R. Joshi, A.A. Jourdain, S.H. Kim, A. V. Kotrys, S.S. Lam, J.G. McCoy, J.D. Meisel, M. Miranda, A. Panda, A. Patgiri, R. Rogers, S. Sadre, H. Shah, O.S. Skinner, T.-L. To, M.A. Walker, H. Wang, P. S. Ward, J. Wengrod, C.-C. Yuan, S.E. Calvo, V.K. Mootha, MitoCarta3.0: an updated mitochondrial proteome now with sub-organellar localization and pathway annotations, *Nucleic Acids Res.* 49 (2021) D1541–D1547, <https://doi.org/10.1093/nar/gkaa1011>.
- [36] T.U. Consortium, UniProt: the universal protein Knowledgebase in 2023, *Nucleic Acids Res.* 51 (2023) D523–D531, <https://doi.org/10.1093/nar/gkac1052>.
- [37] X. Li, Y. Jiang, M. Jill, W. Yang, D.H. Hawke, Y. Zheng, Y. Xia, K. Aldape, J. He, T. Hunter, L. Wang, Z. Lu, Mitochondria-translocated phosphoglycerate kinase 1 functions as a protein kinase to coordinate glycolysis and TCA cycle in tumorigenesis, *Mol. Cell.* 61 (2016) 705–719, <https://doi.org/10.1016/j.molcel.2016.02.009>.
- [38] D.C. Liemburg-Apers, P.H.G.M. Willems, W.J.H. Koopman, S. Grefte, Interactions between mitochondrial reactive oxygen species and cellular glucose metabolism, *Arch. Toxicol.* 89 (2015) 1209–1226, <https://doi.org/10.1007/s00204-015-1520-y>.
- [39] S. Venkat, C. Gregory, J. Sturges, Q. Gan, C. Fan, Studying the lysine acetylation of malate dehydrogenase, *J. Mol. Biol.* 429 (2017) 1396–1405, <https://doi.org/10.1016/j.jmb.2017.03.027>.
- [40] T.M. Durcan, M.Y. Tang, J.R. Pérusse, E.A. Dashti, M.A. Aguilera, G. McLelland, P. Gros, T.A. Shaler, D. Faubert, B. Coulombe, E.A. Fon, USP8 regulates mitophagy by removing K6-linked ubiquitin conjugates from parkin, *EMBO J.* 33 (2014) 2473–2491, <https://doi.org/10.15252/embj.201489729>.
- [41] Y. Liu, C. Guardia-Laguarta, J. Yin, H. Erdjument-Bromage, B. Martin, M. James, X. Jiang, S. Przedborski, The ubiquitination of PINK1 is restricted to its mature 52-kDa form, *Cell Rep.* 20 (2017) 30–39, <https://doi.org/10.1016/j.celrep.2017.06.022>.
- [42] M.A.A. Mahdy, Skeletal muscle fibrosis: an overview, *Cell Tissue Res.* 375 (2019) 575–588, <https://doi.org/10.1007/s00441-018-2955-2>.
- [43] J.A. Ferreira, A.M. Foley, M. Brown, Sex hormones differentially influence voluntary running activity, food intake and body weight in aging female and male rats, *Eur. J. Appl. Physiol.* 112 (2012) 3007–3018, <https://doi.org/10.1007/s00421-011-2271-y>.
- [44] A. La Colla, L. Pronsato, L. Milanese, A. Vasconsuelo, 17 $\beta$ -estradiol and testosterone in sarcopenia: role of satellite cells, *Ageing Res. Rev.* 24 (2015) 166–177, <https://doi.org/10.1016/j.arr.2015.07.011>.
- [45] J.Q. Chen, M. Delannoy, C. Cooke, J.D. Yager, Mitochondrial localization of ER $\alpha$  and ER $\beta$  in human MCF7 cells, *Am. J. Physiol. Endocrinol. Metab.* 286 (2004) E1011–E1022, <https://doi.org/10.1152/ajpendo.00508.2003>.
- [46] A.L. Hevenor, V. Ribas, T.M. Moore, Z. Zhou, ER $\alpha$  in the control of mitochondrial function and metabolic health, *Trends Mol. Med.* 27 (2021) 31–46, <https://doi.org/10.1016/j.molmed.2020.09.006>.
- [47] B. Barone, L. Napolitano, M. Abate, L. Cirillo, P. Reccia, F. Passaro, C. Turco, S. Morra, F. Mastrangelo, A. Scarpato, U. Amicuzi, V. Morgera, L. Romano, F. P. Calace, S.D. Pandolfo, L. De Luca, A. Aveta, E. Scigiano, M. Trivellato, G. Spena, C. D'Alterio, G.M. Fusco, R. Vitale, D. Arcaniolo, F. Crocetto, The role of testosterone in the elderly: what do we know? *Int. J. Mol. Sci.* 23 (2022) 3535, <https://doi.org/10.3390/ijms23073535>.
- [48] G. Hackett, M. Kirby, R.W. Rees, T.H. Jones, A. Muneer, M. Livingston, N. Ossei-Gerning, J. David, J. Foster, P.A. Kalra, S. Ramachandran, The british society for sexual medicine guidelines on male adult testosterone deficiency, with statements for practice, *World J. Mens. Health.* 41 (2023) 508–537, <https://doi.org/10.5534/wjmh.212027>.
- [49] A. Yuki, R. Otsuka, R. Kozakai, I. Kitamura, T. Okura, F. Ando, H. Shimokata, Relationship between low free testosterone levels and loss of muscle mass, *Sci. Rep.* 3 (2013) 1818, <https://doi.org/10.1038/srep01818>.
- [50] C.M. Peterson, D.L. Johannsen, E. Ravussin, Skeletal muscle mitochondria and aging: a review, *J. Aging Res.* 2012 (2012) 194821, <https://doi.org/10.1155/2012/194821>.
- [51] S.M. Houten, S. Violante, F.V. Ventura, R.J.A. Wanders, The biochemistry and physiology of mitochondrial fatty acid  $\beta$ -oxidation and its genetic disorders, *Annu. Rev. Physiol.* 78 (2016) 23–44, <https://doi.org/10.1146/annurev-physiol-021115-105045>.
- [52] Z. Zhou, J. Zhou, Y. Du, Estrogen receptor alpha interacts with mitochondrial protein HADHB and affects beta-oxidation activity, *Mol. Cell. Proteomics* 11 (2012) 1–12, <https://doi.org/10.1074/mcp.M111.011056>.
- [53] K. Ohlndieck, Proteomic profiling of fast-to-slow muscle transitions during aging, *Front. Physiol.* 2 (2011) 105, <https://doi.org/10.3389/fphys.2011.00105>.
- [54] Y.S. Bae, H. Oh, S.G. Rhee, Y. Do Yoo, Regulation of reactive oxygen species generation in cell signaling, *Mol. Cell.* 32 (2011) 491–509, <https://doi.org/10.1007/s10059-011-0276-3>.
- [55] T. Xu, V. Pagadala, D.M. Mueller, Understanding structure, function, and mutations in the mitochondrial ATP synthase, *Microb. Cell* 2 (2015) 105–125, <https://doi.org/10.15698/mic2015.04.197>.
- [56] E.J. Bhoj, M. Li, R. Ahrens-Nicklas, L.C. Pyle, J. Wang, V.W. Zhang, C. Clarke, L. J. Wong, N. Sondheimer, C. Ficcioglu, M. Yudkoff, Pathologic variants of the mitochondrial phosphate carrier SLC25A3: two new patients and expansion of the cardiomyopathy/skeletal myopathy phenotype with and without lactic acidosis, *JIMD Rep* 19 (2015) 56–66, <https://doi.org/10.1007/98904.2014.364>.
- [57] Y.-J. Kang, J.-I. Yoo, K.-W. Baek, Differential gene expression profile by RNA sequencing study of elderly osteoporotic hip fracture patients with sarcopenia, *J. Orthop. Transl.* 29 (2021) 10–18, <https://doi.org/10.1016/j.jot.2021.04.009>.
- [58] N.D. Amodeo, G. Punzi, E. Obre, D. Lacombe, A. De Grassi, C.L. Pierri, R. Rossignol, AGC1/2, the mitochondrial aspartate-glutamate carriers, *Biochim. Biophys. Acta Mol. Cell Res.* 1863 (2016) 2394–2412, <https://doi.org/10.1016/j.bbarmac.2016.04.011>.
- [59] D. Liu, M.A. Sartor, G.A. Nader, E.E. Pistilli, L. Tanton, C. Lilly, L. Gutmann, H. B. Iglayeger, P.S. Visich, E.P. Hoffman, P.M. Gordon, Microarray analysis reveals novel features of the muscle aging process in men and women, *Journals Gerontol. - Ser. A Biol. Sci. Med. Sci.* 68 (2013) 1035–1044, <https://doi.org/10.1093/gerona/glt015>.
- [60] F. Palmieri, P. Scarfia, M. Monné, Diseases caused by mutations in mitochondrial carrier genes SLC25: a review, *Biomolecules* 10 (2020) 655, <https://doi.org/10.3390/biom10040655>.
- [61] E. Maldonado, S. Morales-Pison, F. Urbina, A. Solari, Aging hallmarks and the role of oxidative stress, *Antioxidants* 12 (2023) 651, <https://doi.org/10.3390/antiox12030651>.
- [62] S. Reeg, T. Grune, Protein oxidation in aging: does it play a role in aging progression? *Antioxidants Redox Signal.* 23 (2015) 239–255, <https://doi.org/10.1089/ars.2014.6062>.
- [63] B. Colom, J. Oliver, F.J. Garcia-Palmer, Sexual dimorphism in the alterations of cardiac muscle mitochondrial bioenergetics associated to the ageing process, *Journals Gerontol. - Ser. A Biol. Sci. Med. Sci.* 70 (2015) 1360–1369, <https://doi.org/10.1093/gerona/glu014>.
- [64] D. Gorni, A. Finco, Oxidative stress in elderly population: a prevention screening study, *Aging Med* 3 (2020) 205–213, <https://doi.org/10.1002/agm2.12121>.
- [65] G. Fanò, P. Mecocci, J. Vecchiet, S. Belia, S. Fulle, M.C. Polidori, G. Felzani, U. Senin, L. Vecchiet, M.F. Beal, Age and sex influence on oxidative damage and functional status in human skeletal muscle, *J. Muscle Res. Cell Motil.* 22 (2001) 345–351, <https://doi.org/10.1023/A:1013122805060>.
- [66] J. Feng, H. Xie, D.L. Meany, L. V. Thompson, E.A. Arriaga, T.J. Griffin, Quantitative proteomic profiling of muscle type-dependent and age-dependent protein carbonylation in rat skeletal muscle mitochondria, *Journals Gerontol. Ser. A Biol. Sci. Med. Sci.* 63 (2008) 1137–1152, <https://doi.org/10.1093/gerona/63.11.1137>.
- [67] K. Szczepanowska, A. Trifunovic, Mitochondrial matrix proteases: quality control and beyond, *FEBS J.* 289 (2022) 7128–7146, <https://doi.org/10.1111/febs.15964>.
- [68] U. Richter, T. Lahtinen, P. Marttinen, F. Suoni, B.J. Battersby, Quality control of mitochondrial protein synthesis is required for membrane integrity and cell fitness, *J. Cell Biol.* 211 (2015) 373–389, <https://doi.org/10.1083/jcb.201504062>.
- [69] J. Wu, J.L. Ruas, J.L. Estall, K.A. Rasbach, J.H. Choi, L. Ye, P. Boström, H.M. Tyra, R.W. Crawford, K.P. Campbell, D.T. Rutkowski, R.J. Kaufman, B.M. Spiegelman, The unfolded protein response mediates adaptation to exercise in skeletal muscle through a PGC-1 $\alpha$ /ATF6 $\alpha$  complex, *Cell Metabol.* 13 (2011) 160–169, <https://doi.org/10.1016/j.cmet.2011.01.003>.
- [70] Y. Cai, H. Shen, H. Weng, Y. Wang, G. Cai, X. Chen, Q. Ye, Overexpression of PGC-1 $\alpha$  influences the mitochondrial unfolded protein response (mtUPR) induced by MPP+ in human SH-SY5Y neuroblastoma cells, *Sci. Rep.* 10 (2020) 10444, <https://doi.org/10.1038/s41598-020-67229-6>.

- [71] Y. Wang, J. Li, Z. Zhang, R. Wang, H. Bo, Y. Zhang, Exercise improves the coordination of the mitochondrial unfolded protein response and mitophagy in aging skeletal muscle, *Life* 13 (2023) 1006, <https://doi.org/10.3390/life13041006>.
- [72] A.P.K. Wodrich, A.W. Scott, A.K. Shukla, B.T. Harris, E. Giniger, The unfolded protein responses in health, aging, and neurodegeneration: recent advances and future considerations, *Front. Mol. Neurosci.* 15 (2022) 831116, <https://doi.org/10.3389/fnmol.2022.831116>.
- [73] S. Wang, H. Long, L. Hou, B. Feng, Z. Ma, Y. Wu, Y. Zeng, J. Cai, D. Zhang, G. Zhao, The mitophagy pathway and its implications in human diseases, *Signal Transduct. Targeted Ther.* 8 (2023) 304, <https://doi.org/10.1038/s41392-023-01503-7>.
- [74] R. Ventura-Clapier, M. Moulin, J. Piquereau, C. Lemaire, M. Mericskay, V. Veksler, A. Garnier, Mitochondria: a central target for sex differences in pathologies, *Clin. Sci.* 131 (2017) 803–822, <https://doi.org/10.1042/CS20160485>.
- [75] J.-P. Leduc-Gaudet, S.N.A. Hussain, E. Barreiro, G. Gouspillou, Mitochondrial dynamics and mitophagy in skeletal muscle health and aging, *Int. J. Mol. Sci.* 22 (2021) 8179, <https://doi.org/10.3390/ijms22158179>.
- [76] C. López-Otín, M.A. Blasco, L. Partridge, M. Serrano, G. Kroemer, The hallmarks of aging, *Cell* 153 (2013) 1194–1217, <https://doi.org/10.1016/j.cell.2013.05.039>.
- [77] D.C. Hughes, L.M. Baehr, D.S. Waddell, A.P. Sharples, S.C. Bodine, Ubiquitin ligases in longevity and aging skeletal muscle, *Int. J. Mol. Sci.* 23 (2022) 7602, <https://doi.org/10.3390/ijms23147602>.